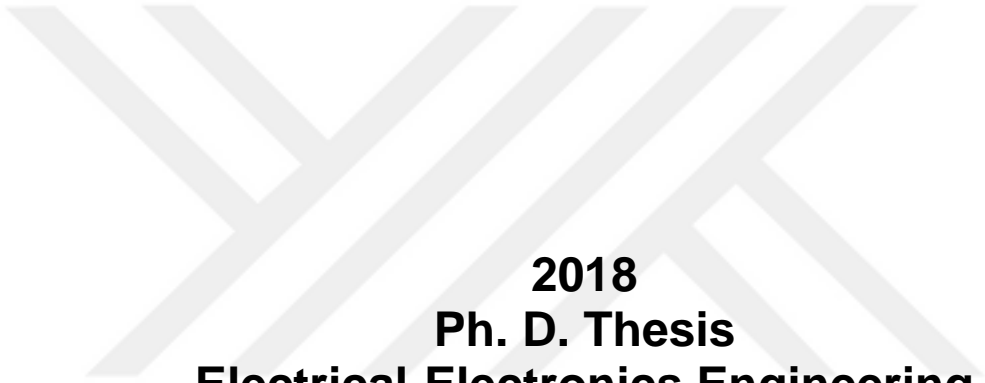


**3 DIMENSIONAL MONOMODAL INTENSITY
BASED MEDICAL IMAGE REGISTRATION FOR
BRAIN TUMOR PROGRESSION ANALYSIS**



**2018
Ph. D. Thesis
Electrical-Electronics Engineering**

EMRAH IRMAK

**3 DIMENSIONAL MONOMODAL INTENSITY BASED MEDICAL IMAGE
REGISTRATION FOR BRAIN TUMOR PROGRESSION ANALYSIS**

**A THESIS SUBMITTED TO
THE GRADUATE SCHOOL OF NATURAL AND APPLIED SCIENCES OF
KARABUK UNIVERSITY**

BY

EMRAH IRMAK

**IN PARTIAL FULFILLMENT OF THE REQUIREMENTS FOR
THE DEGREE OF DOCTOR OF PHILOSOPHY IN
DEPARTMENT OF
ELECTRICAL-ELECTRONICS ENGINEERING**

JANUARY 2018

I certify that in my opinion the thesis submitted by Emrah IRMAK titled “3 DIMENSIONAL MONOMODAL INTENSITY BASED MEDICAL IMAGE REGISTRATION FOR BRAIN TUMOR PROGRESSION ANALYSIS” is fully adequate in scope and in quality as a thesis for the degree of Doctor of Philosophy of Science.

Assist. Prof. Dr. Mustafa Burak TÜRKÖZ

Thesis Advisor, Department of Electrical-Electronics Engineering



This thesis is accepted by the examining committee with a unanimous vote in the Department of Electrical-Electronics Engineering as a Ph. D. thesis. 05/01/2018

Examining Committee Members (Institutions)

Signature

Chairman: Prof. Dr. Ergun ERÇELEBİ (GÜ)



Member : Prof. Dr. Mustafa YILMAZLAR (SAÜ)



Member : Assoc. Prof. Dr. Habibe TECİMER (KBÜ)



Member : Assist. Prof. Dr. Mustafa Burak TÜRKÖZ (KBÜ)



Member : Assist. Prof. Dr. Ahmet Reşit KAVSAOĞLU (KBÜ)



... / ... / 2018

The degree of Doctor of Philosophy of Science by the thesis submitted is approved by the Administrative Board of the Graduate School of Natural and Applied Sciences, Karabük University.

Prof. Dr. Filiz ERSÖZ

Head of Graduate School of Natural and Applied Sciences

.....



“I declare that all the information within this thesis has been gathered and presented in accordance with academic regulations and ethical principles and I have according to the requirements of these regulations and principles cited all those which do not originate in this work as well.”

Emrah IRMAK

ABSTRACT

Ph. D. Thesis

3-DIMENSIONAL MONOMODAL INTENSITY BASED MEDICAL IMAGE REGISTRATION FOR BRAIN TUMOR PROGRESSION ANALYSIS

Emrah IRMAK

Karabük University

Graduate School of Natural and Applied Sciences

Department of Electrical-Electronics Engineering

Thesis Advisor:

Assist. Prof. Dr. Mustafa Burak TÜRKÖZ

January 2018, 58 pages

Brain's Magnetic Resonance (MR) images include anatomic sense for neurologic research, diagnosis and treatment. Therefore to evaluate changes in serial scans of MR images becomes an important issue in cancer research field. The measurement of tumor volume change and tumor progression analysis is a very common task in cancer research. Tumor volume change analysis can be carried out in two ways. First is using different mathematical formulas, second using image registration-segmentation methods. Specifically, image registration is a fundamental job used to match two or more than two images acquired, for example, at different times, from different machines or sensors, or from different viewpoints. In this thesis an objective application of registration and segmentation of multiple brain imaging scans is used to investigate brain tumor growth in a 3 dimensional (3D) manner. Using 3D medical image registration-segmentation algorithm, multiple scans of MR images of a patient who has brain tumor are registered with MR images of the same

patient acquired at a different time so that growth of the tumor inside the patient's brain can be investigated. Brain tumor volume measurement is also achieved using various mathematical formulas to testify the proposed application in this thesis. Medical image registration-segmentation is implemented to 19 patients and satisfactory results are obtained. A challenge of medical image registration-segmentation method for brain tumor investigation is that grown, diminished and unchanged brain tumor parts of the patients are investigated and computed on an individual basis in a three-dimensional (3D) manner within the time. This study is a critical application for correlation of anatomic information obtained by MR for clinical and research purposes. This thesis is intended to supply a comprehensive reference source for the scientists, clinicians and researchers who are interested in medical image registration and tumor growth investigation.

Key Words : Brain tumor growth, medical image registration, tumor volume computing, medical image segmentation.

Science Code : 905.1.021

ÖZET

Doktora Tezi

BEYİN TÜMÖRÜ GELİŞİMİNİN ANALİZİ İÇİN TEK MODLU PİKSEL KOYULUK TEMELLİ 3 BOYUTLU TIBBİ GÖRÜNTÜ ÇAKIŞTIRMA

Emrah IRMAK

Karabük Üniversitesi

Fen Bilimleri Enstitüsü

Elektrik-Elektronik Mühendisliği Anabilim Dalı

Tez Danışmanı:

Yrd. Doç. Dr. Mustafa Burak TÜRKÖZ

Ocak 2018, 58 sayfa

Beynin Manyetik Rezonans (MR) görüntüleri nörolojik araştırma, tanı ve tedavi için anatomik bir anlam içerir. Bu nedenle, MR görüntülerinin seri taramalarındaki değişimleri değerlendirmek kanser araştırmaları alanında önemli bir konu haline gelmiştir. Tümörün hacim ilerlemesi ve tümör değişim hacmi hesaplanması, kanser araştırmalarında çok yaygın bir yer teşkil etmektedir. Tümör hacim değişim analizi iki şekilde gerçekleştirilebilir. Birincisi, literatürdeki çeşitli matematiksel formülleri kullanmak, ikincisi ise görüntü çakıştırma-bölütleme yöntemlerini kullanmaktır. Görüntü çakıştırma farklı zamanlarda, farklı makinelerden veya sensörlerden veya farklı bakış açılarından elde edilen iki veya ikiden fazla görüntüyü üst üste getirmek için kullanılan temel bir işlemdir. Bu tezde, beyin tümörü büyümesini 3 boyutlu (3B) bir şekilde araştırmak için, çoklu beyin görüntüleme taramalarının çakıştırılması ve bölütlenmesi suretiyle objektif bir uygulama yapılmıştır. 3B tıbbi görüntü çakıştırma-bölütleme algoritması kullanılarak, beyin tümörü bulunan bir

hastanın MR görüntüleri, aynı hastadan farklı bir zamanda elde edilen farklı MR görüntüleriyle karşılaştırılır, böylece hastanın beyindeki tümörün büyümesi araştırılmaktadır. Beyin tümörü hacim değişim ölçümü, aynı zamanda bu tezde matematiksel formüllerle de yapılarak önerilen uygulama test edilmektedir. 19 hastaya tıbbi görüntü karşılaştırma-bölütleme yöntemi uygulanmış ve tatmin edici sonuçlar elde edilmiştir. Bu çalışmanın bir diğer ilgi çekici yanı hastaların büyümüş, azalmış ve değişmemiş beyin tümörü parçalarının zaman içinde üç boyutlu (3B) bir şekilde bireysel olarak araştırılıp hacimlerinin hesaplanmasıdır. Bu çalışma MR tarafından elde edilen anatomik bilgilerinin klinik ve araştırma amaçlı korelasyonu için kritik bir uygulamadır. Bu tez, tıbbi görüntü karşılaştırma ve tümör hacmi değişim analizi ile ilgilenen araştırmacılar için kapsamlı bir referans kaynağı sağlamayı amaçlamaktadır.

Anahtar Sözcükler : Beyin tümörü gelişimi, tıbbi görüntü karşılaştırma, tümör hacminin hesaplanması, tıbbi görüntü bölütleme.

Bilim Kodu : 905.1.021

ACKNOWLEDGEMENT

I would like to express my deepest gratitude to my supervisor Yrd. Doç. Dr. Mustafa Burak TÜRKÖZ for his guidance, advice, criticism, encouragements and insight throughout this study.

I would also like to thank to my friend Mehmet BOZDAL for supporting and encouraging me with his best wishes.

Special thanks to my teacher Prof. Dr. Ergun ERÇELEBİ for his kind help, encouragement and patience during my study.

I wish to thank to my sister and her husband, Selma IŞIK and Ercan IŞIK for supporting and encouraging me with their best wishes.

Finally, I would like to thank my parents, Osman IRMAK and Hasibe IRMAK, who have created and maintained a wonderful life for me and contributed to my life with their lovely supports and encouragements.

This work was supported by Scientific Research Projects Coordination Unit of Karabük University. Project Number: KBÜ-17-DR-260 [D6].

CONTENTS

	<u>Page</u>
APPROVAL.....	Hata! Yer işareti tanımlanmamış.
ABSTRACT	iv
ACKNOWLEDGEMENT	viii
CONTENTS	ix
LIST OF FIGURES	xi
LIST OF TABLES	xii
SYMBOLS AND ABBREVIATIONS INDEX.....	xiii
CHAPTER 1	1
INTRODUCTION	1
1.1. HUMAN BRAIN	1
1.2. BRAIN TUMORS	3
1.3. FROM RÖNTGEN TO MAGNETIC RESONANCE IMAGING: THE REVOLUTION OF MEDICAL IMAGING	4
1.4. MEDICAL IMAGING AND MRI.....	5
1.5. IMPORTANCE OF VOLUME DETERMINATION.....	6
1.6. LITERATURE SURVEY	6
1.7. PROBLEM STATEMENT AND CONTRIBUTION OF THESIS	12
1.8. ORGANIZATION OF THESIS	13
CHAPTER 2	15
MATERIALS AND METHODS	15
2.1. MATHEMATICAL MODELS FOR TUMOR VOLUME PROGRESSION ANALYSIS	15
2.2. MEDICAL IMAGE REGISTRATION-SEGMENTATION BASED MODEL.....	18
2.2.1. Geometrical Transformation.....	20
2.2.2. Types of Transformation	21
2.2.2.1. Translation	21

	<u>Page</u>
2.2.2.2. Scaling.....	22
2.2.2.3. Rotation.....	23
2.2.2.4. Shearing	24
2.2.3. Similarity Measure.....	26
2.2.3.1. Sum of Squared Differences (SSD)	26
2.2.4. Optimizer	27
2.2.4.1. Regular Step Gradient Descend Optimizer.....	27
2.2.5. Color Based Image Segmentation of Grown, Diminishing and Unchanged Tumor Parts using L*a*b* Color Space.....	28
2.2.5.1. Color Differences, Delta E Differences and Tolerances.....	30
CHAPTER 3	33
EXPERIMENTAL RESULTS	33
CHAPTER 4	48
CONCLUSION	48
REFERENCES.....	50
RESUME	58

LIST OF FIGURES

	<u>Page</u>
Figure 1.1. An introduction to brain structures, source: wikijournal of medicine.	2
Figure 1.2. Sectional planes of the human brain, source: wikijournal of medicine. ...	3
Figure 1.3. Different medical image modalities for the same patient.	5
Figure 1.4. Frequency of published papers in medical image registration obtained via ISI.	12
Figure 2.1. Visual representation of image registration.	19
Figure 2.2. A simple translation transformation.	22
Figure 2.3. A simple scale transformation.	23
Figure 2.4. Rotation of a point.	23
Figure 2.5. A simple rotation transformation.	24
Figure 2.6. A simple horizontal shear transformation.	25
Figure 2.7. Regular step gradient descend optimizer.	28
Figure 3.1. Fixed image.	34
Figure 3.2. Moving image.	35
Figure 3.3. Overlapping result.	36
Figure 3.4. Registration result.	37
Figure 3.5. Segmented tumor.	38
Figure 3.6. Segmented tumor after filtering.	39
Figure 3.7. Segmented tumor (first patient).	41
Figure 3.8. Segmented tumor (first patient).	42
Figure 3.9. Segmented tumor (second patient).	43
Figure 3.10. Segmented tumor (second patient).	44

LIST OF TABLES

	<u>Page</u>
Table 2.1. Tumor volume measurement formulas.	17
Table 3.1. SSD results with respect to iteration number.	40
Table 3.2. Tumor volume measurement formulas and results.	46
Table 3.3. Tumor size variation results for 19 patients using medical image registration-segmentation method.	47



SYMBOLS AND ABBREVIATIONS INDEX

ABBREVIATIONS

MR	: Magnetic Resonance
MRI	: Magnetic Resonance Imaging
fMRI	: Functional Magnetic Resonance Imaging
CT	: Computed Tomography
PET	: Positron Emission Tomography
SPECT	: Single Photon Emission Computed Tomography
F	: Frequency
TR	: Repetition Time
TE	: Echo Time
TI	: Inversion Time
Flash	: Fast Low Angle Shot
DSP	: Digital Signal Processor
FT	: Fourier Transform
IR	: Image Registration
MATLAB	: Matrix Laboratory
SSD	: Sum of Squared Differences
MI	: Mutual Information
CC	: Cross Correlation
Min.	: Minimum
Max.	: Maximum
Pixel	: Picture Elements
T	: Transformation
2-D	: Two Dimensional
3-D	: Three Dimensional
IQ	: Intelligence Quotient
WHO	: World Health Organization

ICRU : International Commission on Radiation Units and Measurements
L : Length
W : Width
H : Height
VolSph : Volume of Sphere
VolCyl : Volume of Cylinder
VolEll : Volume of Ellipsoid
CIE : International Commission on Illumination
TCIA : The Cancer Imaging Archieve



CHAPTER 1

INTRODUCTION

1.1. HUMAN BRAIN

The brain of the human is the body's single most crucial organ and makes up the central nervous system with the spinal cord. On average, the brain of an adult weighs roughly about 1.2 – 1.4 kg and this is almost about 2% of the whole body weight. Volume of average human brain is around 1260 cm³ in men and 1130 cm³ in women however there is still not a correlation between IQ and brain weight or volume [1]. Human brain comprises of three main parts. First human brain part is known as the cerebrum, the second one as the brainstem and finally the third one as the cerebellum. Brain manages body's different multiple activities such as processing, integrating and coordinating the data that is come from the sense organs. Moreover it makes decisions and sends instructions to the rest of the body. There is the skull bone of the head outside of the brain to protect and surround the brain. Cerebrum which is exactly the biggest part of the brain consists of two cerebral hemispheres. Every single hemisphere is split into 4 important lobes. The outer part of the hemispheres is called cerebral cortex which is also known as grey matter. The ridges staying over the surface of the brain are called gyri and grooves on the surface of the brain are called sulci. These ridges and grooves are generally named according to their positions. Below of the brain is cerebellum resting at the back of the cranial activity. Cerebellum is joined to midbrain of brainstem, to the pons and to the medulla. The cerebellum, the last but not least main part of the human brain, consists of an inner white matter medulla and an outer richly folded grey matter cortex. See Figure 1.1 for the main brain structures.

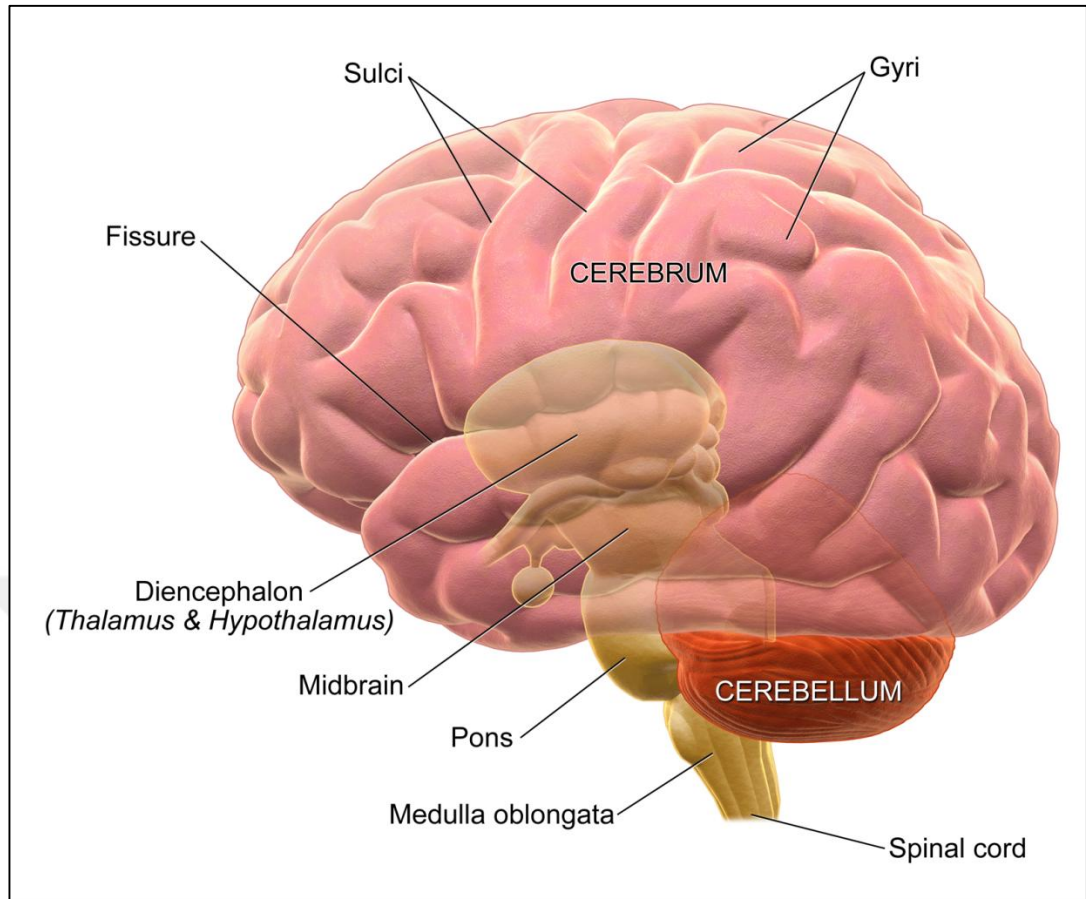


Figure 1.1. An introduction to brain structures, source: wikijournal of medicine.

Three basic reference planes are often used to describe location of the human brain. These planes are Frontal Plane, Sagittal Plane and Transverse Plane. The frontal plane which is also known as coronal plane divides the brain back and front portions. The frontal plane is X-Z plane in terms of rectangular plane. The sagittal plane which is also known as longitudinal is a plane parallel to the sagittal suture. The sagittal plane is Y-Z plane in terms of rectangular plane and it is perpendicular to the ground. This plane, on the other hand, divides the brain right and left portions. The transverse plane which is also known as horizontal plane is cross section that divides the brain head and tail portions. The transverse plane is X-Y plane in terms of rectangular plane. See Figure 1.2 for sectional planes of the human brain.

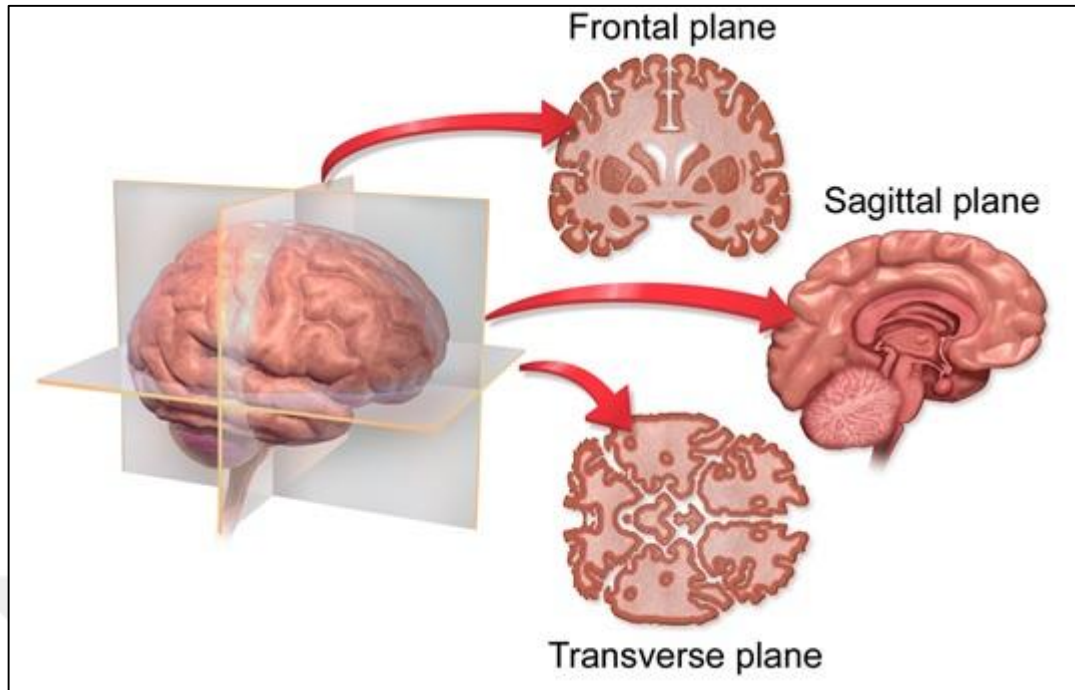


Figure 1.2. Sectional planes of the human brain, source: wikijournal of medicine.

1.2. BRAIN TUMORS

Brain plays a key role in terms of the functioning of the body. This crucial role represents improving treatment protocols which are very important and related to brain tumors or gliomas. Brain tumors have been announced as one of the most fatal cancers in the western population [2]. Moreover, Kohler et al. [3] declared that probability of occurrence of primary tumors of the nervous system or brain is 25 per 100,000. By almost a third are malignant and the remaining are benignant or some kind of benignant. Brain tumors are known as leading death cause among children cancers. In addition to this, they are the second for the males who are between ages of 20-39. Moreover, brain tumors are fifth death cause for the women who are between the ages of 20-39 [4]. World Health Organization (WHO) has introduced a grading scheme which categorizes brain tumors between I and IV. Glioblastoma (WHO grade IV) is known as the most fatal and the most frequent brain tumor which shows very rapid growth [5]. Although treatment methods such as surgery, radiation, chemotherapy are available for treatment of glioblastoma average survival time is 15 months because of the infiltrating nature of glioblastoma [6]. That is why the special care should be given to treatment of glioblastoma. Actually treatment of

glioblastoma becomes one of the most challenging fields in oncology [5]. There is a thriving attention and application of glioblastoma progression analysis in clinical diagnostics and analysis. Thanks to the big amount of data the principal focus of this thesis will be on MRI and glioblastoma tumor volume change calculation.

1.3. FROM RÖNTGEN TO MAGNETIC RESONANCE IMAGING: THE REVOLUTION OF MEDICAL IMAGING

Medical imaging is a technical approach to generate informative images from the human body for the sake of clinical purposes. Medical imaging is a sort of mathematical inverse problems because it is commonly perceived to specify the series of methods that noninvasively generate images belonging to body's internal aspect. History of medical imaging goes along way back to November 1895 with Wilhelm Conrad Röntgen's discovery of X-ray. Wilhelm Conrad realized that invisible light were able to pass through solid parts of human body (e.g. human flesh) more than other parts (e.g. human bone). Because of this discovery, medical imaging is considered to be found with the invention of X-ray. Wilhelm Conrad Röntgen realized that his bones were visible on a photographic plate placed on an electron beam tube in November 1895. Röntgen concluded his experiment when he saw bones of his wife's hand too [7]. Röntgen's technology was proofed after a number of experiments conducted in different parts of world such as in Europe and America. Nowadays clinicians or radiologists can easily image and investigate human body in details using various imaging technologies such as magnetic resonance imaging, ultrasound, radiography, nuclear medicine, computed tomography, tactile imaging, photoacoustic imaging, positron emission tomography etc. Screening, diagnosis and monitoring of disease have been remarkably improved thanks to these technologies. For instance, positron emission tomography which is a trending topic within the imaging modalities can now endow with tumor activity information. Ultrasound, on the other hand, is commonly used to provide needed monitoring of a fetus in due course of pregnancy. Mammography is now the primary technique for breast cancer imaging. Nuclear medicine became quite important after the advancements of magnetic resonance imaging, radiography, positron emission tomography and computed tomography. Diagnoses of central nervous system diseases (cerebrum and

spinal cord), sports injuries, musculoskeletal system problems, meniscus injuries, spinal disc herniation problems, neurologic diseases are basic diseases and problems which MR and other medical imaging techniques deal with. Figure 1.3 shows different medical imaging techniques which are quite popular in medicine.

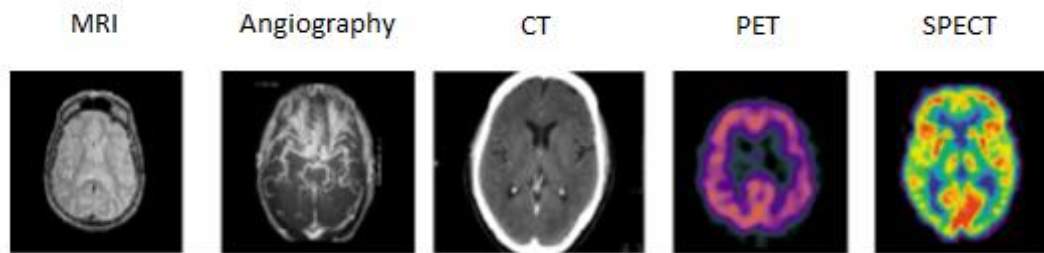


Figure 1.3. Different medical image modalities for the same patient.

1.4. MEDICAL IMAGING AND MRI

Magnetic Resonance (MR) can be considered as one of the main and early medical imaging techniques with the X-ray to investigate the anatomy and function of human body. With the aid of high level magnetism and reflection method the living tissue is visualized. Indeed, the technique which is known as MR is nuclear magnetic resonance imaging. The image is created according to the density and mobility of the hydrogen atoms inside the living tissues. Nowadays MR is particularly used for imaging of soft tissues. Various researchers have showed that MRI is superior to CT for diagnostic brain imaging [8–11]. Magnetic resonance imaging is a quite standard, very popular, useful, practical and non-invasive technique at the same time. In addition MRI is widely available in clinics. Consequently, MRI together in combination with other medical imaging modalities based studies is more feasible and rational in a clinical point of view. Nevertheless, it should be kept in mind that for a final decision and diagnosis, biopsy and histology are necessary despite the all suitability and practicability of non-invasive imagings. Thanks to the big amount of data the principal focus of this thesis will be on MRI and glioblastoma tumor volume change calculation.

1.5. IMPORTANCE OF VOLUME DETERMINATION

It is quite important for the radiologists and/or clinicians to see the volume changes of the brain tumor for neurologic research, diagnosis and treatment plan. These subject matters for the brain tumor are applicable only if the related volume can be implicitly identified and only then tumor volume can be calculated. Glioblastoma is a notably deadly disease today and even today's treatment modalities are all around insufficient in curing or even controlling. In radiotherapy, X radiation of high amount is used to damage and annihilate cancerous cells in the brain. This is applicable only if the related volume can be implicitly identified. Namely the aim of radiotherapy can be seen as powerfully irradiate the tumor area and consequently the target volume but one has to prevent related radiation dose absorbed by nearby healthy cells. Different radiation dose is delivered to different volumes. International Commission on Radiation Units and Measurements (ICRU) introduced ICRU 50 reports which explain the different volumes to be used for radiation treatment planning to keep away from uncertainty in definition of target volumes [4]. One deficiency of today's brain radiotherapy methods is an incompetency to satisfyingly irradiate the target volume to destroy cancerous cells. Glioblastomas are comparatively resistant to X radiation in comparison with other tumor types. Scientists have introduced that most brain tumor which had reoccurred within the time are seemed to be located inside the primary tumor area [12–15]. Although there are studies on measuring the volume of the brain tumor, the definition of brain tumor volume still depends on time consuming, quite based on manual outlining by radiologists, clinicians etc. [4]. Today's treatments for glioblastoma ordinarily need tumor removal using surgical methods.

1.6. LITERATURE SURVEY

Various researchers have studied tumor volume investigation by both measuring and calculation [14–19]. Tumor volume measurement is done by a lot of techniques such as 3D I-scan, ultrasonic 3D scanning system, correlation, diameter, height, area calculation etc. These techniques can be mainly classified into two groups; medical image processing based models and mathematical models [15,16].

For mathematical models, tumor volume calculation is achieved by using various mathematical formulas [16–18]. Guthoff [19], for example, made use of area of sphere phenomena, however the usage of that methods was not sustainable now that it was found to be too complicated. Char et al. [16] searched growth rate using an exponential growth model with tumor volume formula. Difference in tumor size with respect to time was considered as growth rate. Li et al. [17] considered the tumor volume as a part of spheroid intersected by a sphere with a very detailed formula. Many researchers believed the change in tumor diameter to be model for the whole brain tumor volume [20–22]. These researchers found it enough to measure only one dimension of the tumor. On the other hand some researchers measured average of two dimensions [23,24]. Others considered the volume to be proportional to area and measured tumor area from measurements of two perpendicular diameters. E. Richtig et al. [18] investigated that tumor volume, calculated by the easy to use formula of the half volume of a rotation ellipsoid, rotated around the y-axis, is a better than tumor diameter or tumor height.

For medical image processing based models, a wide range of medical image techniques have been presented with the developments in medical image processing field over the years. As these techniques were independently studied, a large body of research is evolved. As far as it goes there are quite a large number of techniques. However, now that every method is designed for a specific application rather than specific types of problems, categorizations and comparison of techniques with each other become difficult. Fortunately calculation was made using medical image segmentation, medical image registration and the combination of segmentation and registration. Medical image registration with segmentation is very important for monitoring glioblastomas growth during therapy as well as glioblastoma tumor volume measurement. Since the year of 2000, a very large number of academic and scientific manuscripts have been showing the growing interest and application of medical image processing [25–28]. See Figure 1.4 for frequency of publications in medical image registration field between years 2000 to 2014. Brock et al. [29] used a deformable registration method for tumor registration. The drawback was the substantial processing time. Kaus et al. [30] explored a new surface-based technique and applied on human brain. This researcher accomplished a few seconds of

processing time but to manually select control point was quite complicated and tedious. Maxwell's demons registration was used with lesion growth model by Cuadra et al. [31]. Bloch et al. [32] applied morphology operators to brain diagnosis. However image variations which comes from the outliers such as, size, noise and feature shapes affected to these operators which are used by the author [25]. Wavelet based methods are getting increase in medical image registration for brain tumor analysis. There are highly various implementations of the wavelets in medical image registration for medical diagnosis [33–38]. The neural network have the ability of predicting, analyzing and deriving useful related information from a given data therefore this ability makes the neural network attractive to image registration for brain cancer diagnosis [25]. Konukoglu et al. [39] made use of a very useful registration technique which involved tumor segmentation, image registration and change detection to be able monitor slowly growing brain tumors. Pohl et al. [40] suggested to perceive differences in slowly evolving brain tumors using segmentation, registration and final analysis of differences. Angelini et al. [41] used affine registration to compute and compare intensity difference maps directly for tumor growth.

Image registration is a leading-edge for image processing because rewarding complex data is transported in more than one image which may be obtained at various timelines, from different perspectives or even by totally separate sensors. That is why proper alignment of the beneficial information coming inside two images is very useful for clinical purposes. Besides, preoperative and intraoperative medical image registration is a critical process for image-guided therapy.

A wide range of medical image techniques have been presented with the developments in medical image processing field over the years. As these techniques were independently studied, a large body of research is evolved. Fortunately, techniques differ in information on which registration relies. To put it briefly, connection between the changes of the images and type of the registration method that is most appropriate should be established by the researchers or scientists [42]. Changes points to the volumetric changes of the values and locations of pixels

among the two images [43]. Value changes are generally differences in intensity. The changes in question can be classified in three major types.

The first type is the changes which result in misalignment of the images such as the differences in acquisition. For registering images in question, a spatial transformation is used to cut out these changes. The type of transformations that should be sought to find the optimal transformation is established by gain insight about the changes of this type. The transformation type then affects the general method which should be used. The second type of changes is quite similar to first type because they are also due to changes in acquisition. One of the difference between them is that they cannot be modeled easily, for the sake of example; lighting and atmospheric conditions. Another difference is that this type usually changes intensity value. The third type is changes in the nature of the images, for example tumor growths, or other scene changes. For the medical purposes such as, diagnosis, treatment or neurologic research changes of the third type must not be removed by registration. Therefore third type causes registration to be more challenging because an exact match is not possible anymore [44]. The characteristics of the each type of changes should be taken into account since knowledge about the characteristics of each type of change establishes the choice of feature space, similarity metric, search space and search strategy. Ultimately these all together will establish the main method to be used for registration process for the sake of neurologic research, treatment, diagnosis, etc. This course of action is quite practical for understanding relationships between the large number of existing methods and to be helpful to choose the most appropriate method for the specific purpose.

Within the image registration methods the first widely-used method is point-based (fiducial markers) registration method. Aforementioned registration method is managed via getting the rigid transformation which collects the fiducial points into two spaces into alignment [45]. Promptness, accuracy and robustness are important advantages of point-based registration method. However it requires fixation of fiducial markers to rigid structures, which is not always possible or is too invasive to be acceptable.

Second widely-used method is surface-based registration method. This method is based on an identification of the shape of an anatomical structure. This anatomical structure may be skin or outer bone surface. To be able to estimate registration transformation minimizing points-to-surface or surface-to-surface distances is used. Unfortunately skin is not a rigid structure and that bone surface has to be exposed during the procedure.

Third widely-used method is intensity-based registration method. This technique works directly with image data. Just as almost all the registration techniques to register and process medical images all the associated images must be converted into the digital form, which are originally in analog form. This means that the images must be in number which represents the intensity value of each pixel in the images. Each intensity value in the images refers to color of corresponding location inside the images [46]. Recently intensity-based registration method has grown compare to other methods. There are a few reasons for this situation. Firstly, twenty years ago it was taking hours or even days of computers for registering two image volumes if intensity-based registration method is used. At the present time, a few minutes or even seconds in some situations is enough for a simple computer to be able solve the same intensity-based registration problems. Therefore advances about computational resources, processing speed has led intensity-based registration method over other methods. Secondly, before introduction of similarity measures in intensity-based methods there was not a robust similarity metric to compare the interpolated image as the result of registration process. Namely, with introduction and development of similarity measure, especially mutual information (MI), there has been a considerable development in usage of intensity-based image registration as well. Thirdly, the simplicity of intensity based registration techniques among the remaining techniques encourages the researchers involved in medical image registration to make use of intensity based methods. Not having to struggle with image segmentation which is usually open to making mistakes and is generally complex, is an important result of the simplicity of this method [42].

Looking at literature of medical analysis it can be easily seen that image registration builds up much of the research. Li et al. [47] is worth to be read to consider medical

image registration using mathematical tools. Most of the work related to medical image registration is about registration of functional medical images with anatomical medical images. Positron emission tomography (PET) or functional magnetic resonance imaging (fMRI) is functional medical images which give information about functionality of the human body. On the other hand magnetic resonance imaging (MRI) and computed tomography (CT) are anatomical medical images which give information about anatomy of the human body. By registering two different images a new medical image which contains both anatomical and functional information about human body is much more informative and useful. There are a lot of works in literature about this issue: Gering et al. [48] and Pereira et al. [49] are must read papers for intervention and treatment planning. Chang et al. [50] studied a good case for computer-aided diagnosis and disease following-up. For guided surgery on the other hand, Hurvitz and Joskowicz [51], Huang et al. [52] and Galloway et al. [53] are some the best papers. Ozsavas et al. [54], Mendrik et al. [55], Zhuang [56] and Oliveira et al. [57] made a great effort about anatomy segmentation. Recent improvements have been more on monomodal medical image registration rather than multimodal medical image registration. Acquisition of temporal image sequences contains much of the monomodal image registration research. Compared to multimodal images, mentioned sequences propose additional information about the changes of the imaged organs, such as tumor growths in any part of human body. Object lessons of temporal image registration of the heart can be found in Perperidis et al. [58], Marinelli et al. [59] and Peyrat et al. [60]. Despite that nearly entire anatomic parts and organs of the human body have been studied, much of the research of monomodal image registration has been done on brain. Duay et al. [61], Studhole et al. [62], Liao and Chung [63], Cho et al. [64] and Yazdani et al. [65]. A certain number of reviews on medical image registration such as Pluim et al. [66] Salvi et al. [67], Wyawahare et al. [68], Slomka and Baum [69], Francisco P.M. Oliveira and João Manuel R.S. Tavares [42] can be examined in detail.

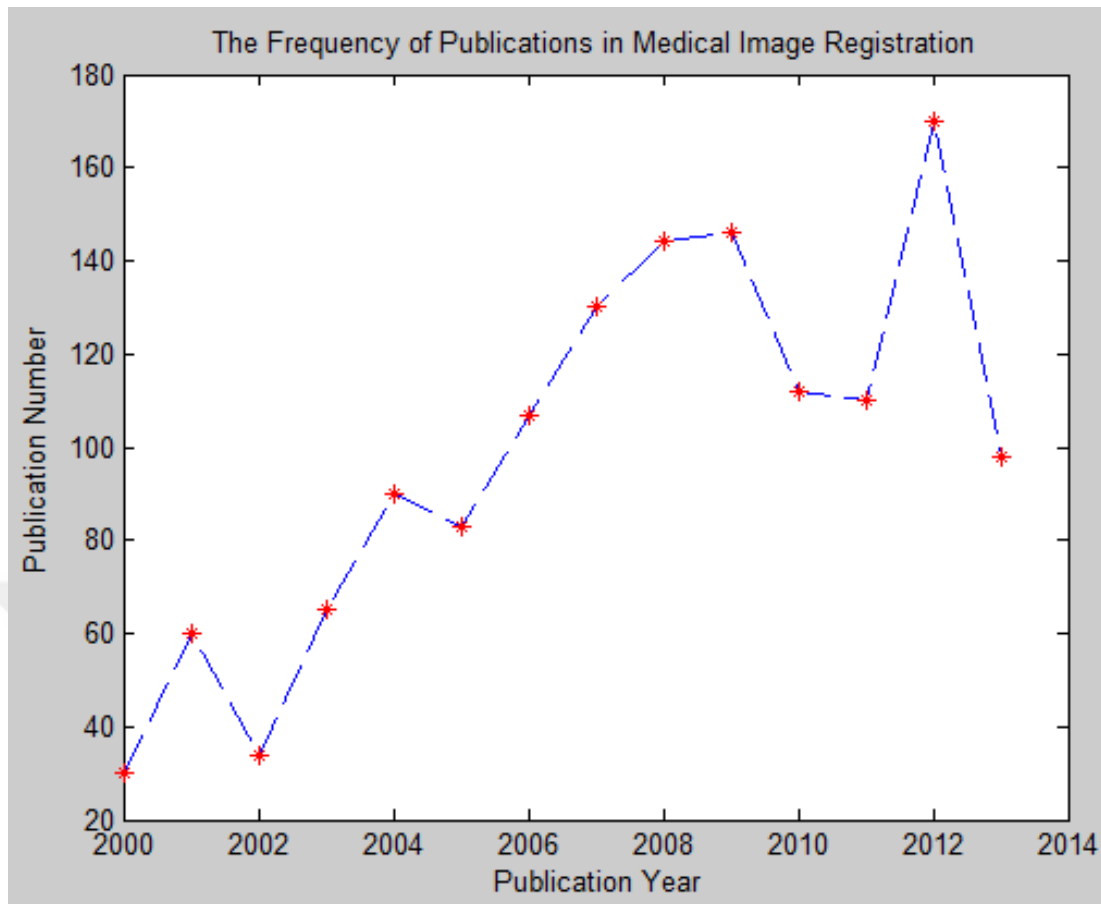


Figure 1.4. Frequency of published papers in medical image registration obtained via ISI.

1.7. PROBLEM STATEMENT AND CONTRIBUTION OF THESIS

It is quite important for the radiologists and/or clinicians to see the volume changes of the brain tumor for neurologic research, diagnosis and treatment plan. Neurologic research, diagnosis and treatment for the brain tumor are applicable only if the related volume can be implicitly identified and tumor volume can be calculated.

Each medical image from different modality or each medical image from the same modality gives unique data and of generally a complementary nature, convenient integration and combination of information gained and collected from separate images is intended. This process is called registration and the goal is to bring images from different modalities or images from same modalities to the spatial alignment. Hence, the problem statement is the requirement of an effective and easy way of

aligning two medical images (MR/MR), taking those medical images to the same coordinate system so that corresponding features can easily be related. Soon after corresponding features are related, the brain volume must be calculated.

A contribution of this thesis is that grown, diminished, and unchanged brain tumor parts of the patients are investigated, segmented out and their volumes are computed on an individual basis in a three-dimensional (3D) manner within the time. It is investigated experimentally that in the case of tumor changing, how much brain tumor grows, how much brain tumor diminishes, or how much brain tumor stays the same using color information. Green parts shows tumor which has been growing with time. Magenta parts, on the other hand, shows tumor which has been diminishing parts with time and lastly white parts are unchanged brain tumors. In literature, three-dimensional volume investigation, not volume calculation, is studied just using three planes (three slices) of the brain tumor. However, it is well-known that brain tumor is a three dimensional phenomenon. That is why not only three slices of tumor but also all the tumor associated slices must be processed.

1.8. ORGANIZATION OF THESIS

This thesis composes of four chapters. Chapter 1 presents overall and well-known information about human brain and brain tumors. Some statistical data about glioblastoma brain tumor is given in this chapter. Moreover, historical background of the medical imaging in medicine is discussed. The question ‘Why is brain tumor volume change so important’ is addressed. Problem statement, contribution of the thesis and a detailed literature survey can be found in Chapter 1. Chapter 2 introduces material and methods. Mathematical based methods and medical image processing method are demonstrated in this chapter. In addition to this, the proposed medical image processing method is presented in detail. Medical image registration and medical image segmentation concepts are discussed and formulated in this chapter. The proposed algorithm for brain volume change investigation is itemized. Chapter 3 demonstrates experimental results obtained from the experiments. Registered and fused MR images are showed and brain volume change results are

given in this chapter. Lastly Chapter 4 is the conclusion part of the thesis. Results and outcomes are commented and possible future work is presented in this chapter.



CHAPTER 2

MATERIALS AND METHODS

2.1. MATHEMATICAL MODELS FOR TUMOR VOLUME PROGRESSION ANALYSIS

There exist important mathematical models for tumor volume progression analysis. Various studies have showed that three dimensional fundamental shape of brain tumor is hemi-ellipsoid [70]. Three dimensions of the tumor measurement are necessary for tumor volume calculations. These are: length (L), width (W), height (H). Measurement of tumor volume is a very common task in brain cancer research. Conventional ellipsoid volume is known as;

$$V = \frac{\pi}{6} * (length) * (width) * (height) \quad (2.1)$$

Although measuring length and width of brain tumor is possible, height measuring is quite problematic. Because when measuring tumor height, there mainly exists inaccuracy which causes the largest error to volume results. The difficulty is determination where to position the caliper for measuring a precise height measurement [71]. That is why some authors have reduced essential number of dimensions in order to measure tumor volume. John P. Feldman et al. [71] explored a new mathematical method for tumor measurement which uses just two dimensions; length and width. There are other researchers who use two or even one dimension for measuring brain tumor. Although measuring brain tumor using 2 dimensions (2D) has been traditionally used one dimensional (1D) measurements have recently recommended. For 2D dimensional estimations one of the dimensions is the longest diameter of the tumor in the MR slices whereas the other dimension is the longest diameter perpendicular to the first dimension. For 1D estimations, on the other hand, the only dimension is the sum of the longest diameters of tumors. Mathematical

measurements of brain tumor are also known as linear measurement based formulae. The simplest one is sphere volume assumption formula which uses just 1D linear measurement for measuring tumor volume. For this purpose the conventional formula is $\text{VolSph} = \frac{4}{3} \pi \left(\frac{1D}{2}\right)^3$. A brain tumor volume can also be assumed as a cylinder when using two orthogonal dimensions for measuring tumor volume. For this assumption the traditional formula is $\text{VolCyl} = \pi \left(\frac{a}{2}\right)^2 b$. Besides, an ellipsoid volume assumption would probably be more accurate. $\text{VolEll} = \frac{4}{3} \pi \frac{a}{2} \frac{b}{2} \frac{c}{2}$ which is a 3D linear measurement. For the 3D measurement estimations, one of the dimension is the longest diameter of tumor, the second dimension is again the longest diameter orthogonal to the first dimension and the last one is the longest diameter which is orthogonal to both of the dimensions.

Table 2.1 shows a lot of mathematical formulas which have been used for tumor volume calculation up to now.

Table 2.1. Tumor volume measurement formulas.

Formula Used	Volume Type	Assumption
$\frac{\pi}{6} * L * W * H$	Ellipsoid	3 Dimensions are proportional wrt tumor growth
$\frac{\pi}{6} * L * W^2$	Ellipsoid	H = W
$\frac{\pi}{6} * \left[\frac{L+W}{2}\right]^3$	Ellipsoid	H = A nonlinear function in terms of L and W
$\frac{\pi}{6} * (L * W)^{\frac{3}{2}}$	Ellipsoid	$H = \sqrt{L * W}$
$0.4 * L * W^2$	Spheroid	$H = \frac{L^2 * W^2}{\pi}$
$\frac{4}{3} * \pi * \left(\frac{L+W}{2}\right)^3$	Spheroid	$r = \frac{L+W}{2}$
$\frac{4}{3} * \pi * \left(\frac{L}{2}\right)^3$	Spheroid	$r = \frac{L}{2}$
$L * W * H$	Rectangular Solid	3 Dimensions are proportional wrt tumor growth
$L * W^2$	Rectangular Solid	H = W
$\frac{1}{2} * L * W * H$	Ellipsoid	$\pi = 3$
$\frac{1}{2} * L * W^2$	Ellipsoid	H = W
$L * W$	Areal	Area proportional to volume
$\frac{\pi}{4} * L * W$	Areal	Area proportional to volume
L	Diameter	Diameter to be representative to volume
$\frac{L+W}{2}$	Diameter	Diameter to be representative to volume

M. M. Tomayko and C.P. Reynolds [72] showed that tumor volume calculation using three-dimensional formula results in the most accurate tumor volume. All the tumor

volume measurement formulas are reasonable good at estimating brain tumor but the formula $\frac{\pi}{6} * (length) * (width) * (height)$ stood out as the best.

2.2. MEDICAL IMAGE REGISTRATION-SEGMENTATION BASED MODEL

Medical image processing techniques, specifically image registration and image segmentation can be used for brain tumor volume measuring and brain tumor volume progression analysis. Image registration is a leading-edge for image processing because rewarding complex data is conveyed in more than one image which may be obtained at various timelines, from different perspectives or even by totally separate sensors. That is why proper alignment of the beneficial information coming from two images is very useful for clinical purposes. Besides, preoperative and intraoperative medical image registration is a critical process for image-guided therapy. In this section of the thesis, well-known definition and general concepts image registration and image segmentation are presented. In addition, proposed algorithm for the intended application is specified. Theoretical background of image registration and image segmentation is explained in detail.

To summarize registration process, Figure 2.1 is an ideal illustration of how process works. It should be stated that the objective is to search repeatedly for a geometrical transformation which optimizes the similarity metric once implemented to moving images. Image which is not changed during registration is called fixed image, the image which is changed, i.e. transformed during registration is called Moving image. The objective of a similarity metric is to establish a value promising how well two images correlate [73]. Role of optimizer is to define search strategy for the process. Interpolator is used to update pixel intensity values in the new coordinate system with respect to the geometrical transformation found previously. Interpolator measures the value of intensity difference between the images in the new positions.

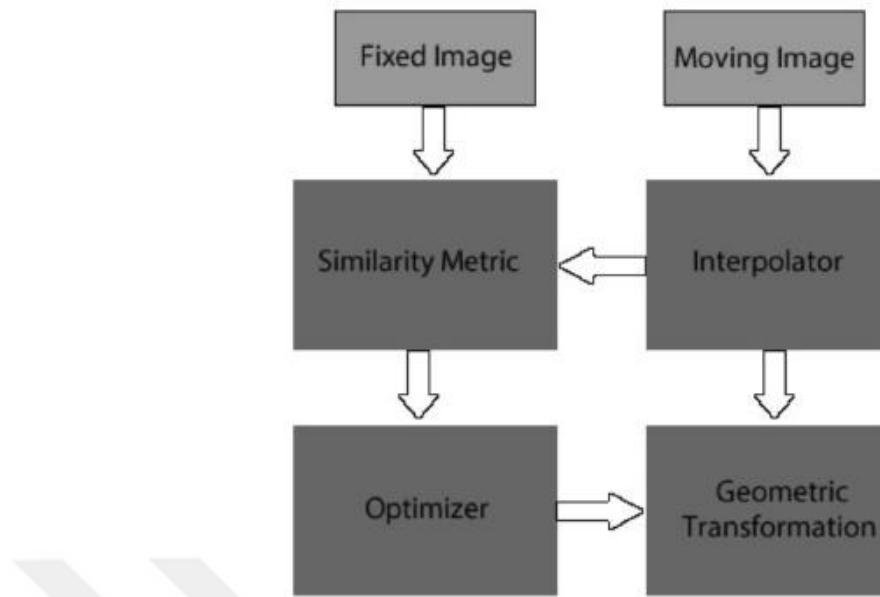


Figure 2.1. Visual representation of image registration.

In this part of the thesis the basic and the simplest mathematical theory of the registration problem are given. Medical image registration strategy can be drawn up as following: To begin with, the type of the transformation is specified. Determining the type of the transformation is a good starting point to help in selecting registration method. On the other hand, transformation itself depends upon the cause of the misalignment. Furthermore, feature space is indicated. Feature space is the intrinsic information of the image. This space is image information space by which similarity measure is computed. Last but not least, similarity measure (metric) is selected. Similarity metric should be most likely to find the best match between fixed image and moving image. On top of that, optimization type is picked up to guide the search to the best match of the fixed and transformed moving image. Finally search techniques are selected to decrease the cost of computations. If possible as a pre-treatment, a pre-registration should be performed for the registration process to bring the fixed and moving images close to each other in the new coordinate system and to provide a faster convergence of the optimization process. This additional algorithm will decrease the possibility of convergence for a local optimum.

2.2.1. Geometrical Transformation

Image registration process has a variety of characteristics. Transformation type is one of the basic characteristic of the image registration in order to properly overlay fixed and moving images. In this part of the thesis procedure of selecting the transformation type for our specific application is explained. Affine transformation is an efficient transformation type for this problem. Now that an affine transformation is composed of a combination of a translation, a rotation, a scale and a shear change. Possible misalignment for MR images taken at different type with the same sensors are translation, rotation scale and shear change. Affine transformation is among the most used transformation types because it is highly sufficient to map two different images of a scene gained from similar angle but at different times.

It is convenient to start by considering linear functions x , y and transformations defined by x and y functions. These transformations might be applied to a point $P(x, y)$ within a plane. All linear transformations T might be represented using following equations:

$$x' = ax + by + e \quad (2.2)$$

$$y' = cx + dy + f \quad (2.3)$$

The point $Q(x', y')$ is called image of P under the transformation T . It is written as, $Q = T(P)$. Two equations can be written in matrix form as follow:

$$\begin{bmatrix} x' \\ y' \end{bmatrix} = \begin{bmatrix} a & b \\ c & d \end{bmatrix} \begin{bmatrix} x \\ y \end{bmatrix} + \begin{bmatrix} e \\ f \end{bmatrix} \quad (2.4)$$

Two equations can also be written as $Q = MP + \vec{v}$, where M and \vec{v} are:

$$M = \begin{bmatrix} a & b \\ c & d \end{bmatrix}, \quad \vec{v} = \begin{bmatrix} e \\ f \end{bmatrix} \quad (2.5)$$

Therefore the product of the matrix M and point P yields MP, and the addition of vector \vec{v} and product MP results in a point that is geometrically the transportation of the point by the magnitude and orientation of the vector.

2.2.2. Types of Transformation

2.2.2.1. Translation

Within the plane, a translation can be generated by setting the transformation matrix M to the identity matrix I and adding \vec{v} to the intended translation.

$$I = \begin{bmatrix} 1 & 0 \\ 0 & 1 \end{bmatrix} \quad (2.6)$$

Translation is quite simple however it has many properties to be discussed. For instance, translation preserves angles which are between lines of the registered images, for this reason we say that parallelism is preserved under translation transformation. This means that the parallel lines within the images, shapes etc. remain parallel after the translation [74]. Translation preserves distances as well as angles; this means that areas of the associated images are also preserved. Simply, we can say that translation is a process of transportation of the images without any physical change. See Figure 2.2 for representation.

$$X = x + h \quad (2.7)$$

$$Y = y + k \quad (2.8)$$

$$\begin{bmatrix} X \\ Y \\ 1 \end{bmatrix} = \begin{bmatrix} 1 & 0 & h \\ 0 & 1 & k \\ 0 & 0 & 1 \end{bmatrix} \begin{bmatrix} x \\ y \\ 1 \end{bmatrix} \quad (2.9)$$

Our goal is to find parameters h and k which are the transformation parameters. The next question is how to find transformation parameters. Knowing a pair of corresponding points in the images, parameter h and k can be determined. In the case

of having more than one pair of corresponding points in images, h and k will be determined using a robust estimator.

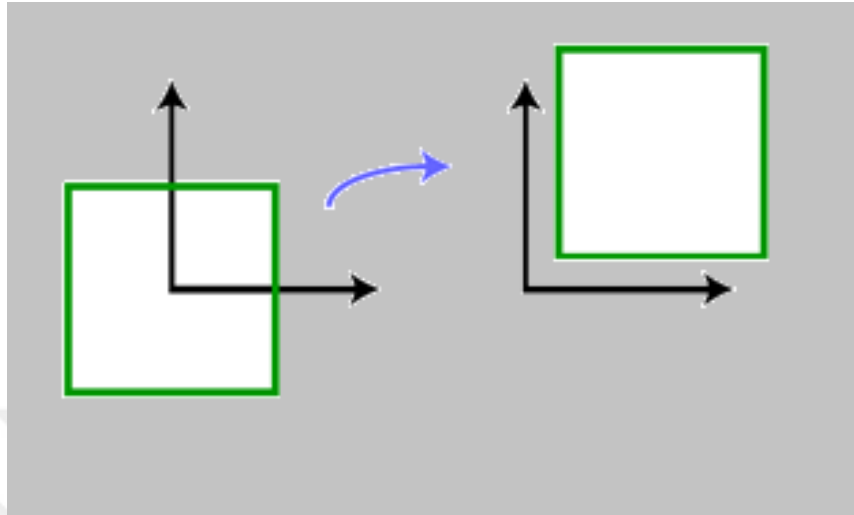


Figure 2.2. A simple translation transformation.

2.2.2.2. Scaling

Scaling transformation can be generated by applying a factor k to the identity matrix I . As we clearly see in Figure 2.3, in scaling transformation angles and parallelism are preserved but areas are not. Let us assume that a matrix, multiplied by a k factor,

$$\begin{bmatrix} k & 0 \\ 0 & k \end{bmatrix} \quad (2.10)$$

is utilized to scale a closed figure. New area after scaling is k^2 times its area before scaling. Figure 2.3 shows geometrically that area is not preserved under scale transformation.

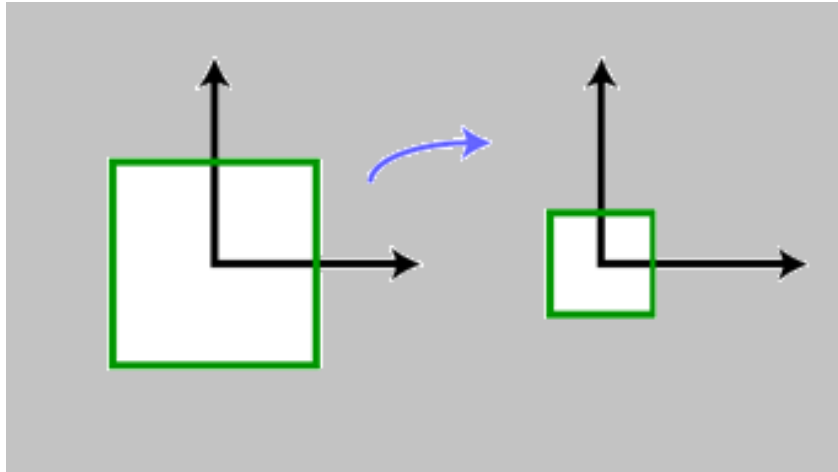


Figure 2.3. A simple scale transformation.

2.2.2.3. Rotation

When speaking about rotation its simplest form is considering rotation about origin. We think that there is a point $P(x, y)$ in Cartesian Coordinates but for simplicity we convert that point into polar coordinates as $P(r\cos(\Theta), r\sin(\Theta))$. And then we applied rotation transformation by angle ϕ to this point. The coordinates of the rotated point $P'(x', y')$ is $(r\cos(\Theta + \phi), r\sin(\Theta + \phi))$ in polar coordinates. See Figure 2.4 below.

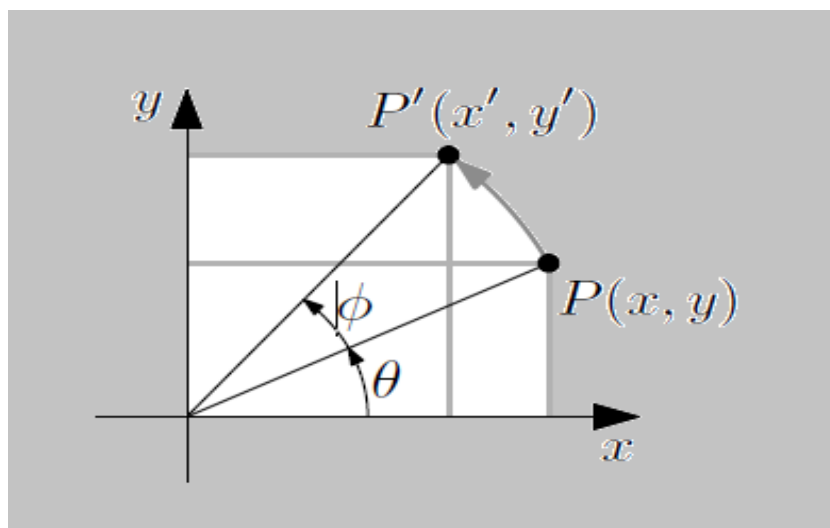


Figure 2.4. Rotation of a point.

Now that,

$$x' = r\cos(\Theta+\varnothing) = r(\cos\Theta\cos\varnothing - \sin\Theta\sin\varnothing) \quad (2.11)$$

$$y' = r\sin(\Theta+\varnothing) = r(\cos\Theta\sin\varnothing + \sin\Theta\cos\varnothing) \quad (2.12)$$

a rotation by an angle \varnothing can be expressed in matrix form as

$$\begin{bmatrix} x' \\ y' \end{bmatrix} = \begin{bmatrix} \cos\varnothing & -\sin\varnothing \\ \sin\varnothing & \cos\varnothing \end{bmatrix} \begin{bmatrix} r\cos\Theta \\ r\sin\Theta \end{bmatrix} = \begin{bmatrix} \cos\varnothing & -\sin\varnothing \\ \sin\varnothing & \cos\varnothing \end{bmatrix} \begin{bmatrix} x \\ y \end{bmatrix} \quad (2.13)$$

We can conclude that the determinant of a rotation transformation matrix is always 1.

$$|M| = \begin{vmatrix} \cos\varnothing & -\sin\varnothing \\ \sin\varnothing & \cos\varnothing \end{vmatrix} = 1. \quad (2.14)$$

Our goal is again to find transformation angle \varnothing . This angle can be calculated if we know a pair of corresponding points in the images. One important note is that if the counterclockwise rotation is the point in question, the transpose of the transformation matrix should be used instead of above matrix.

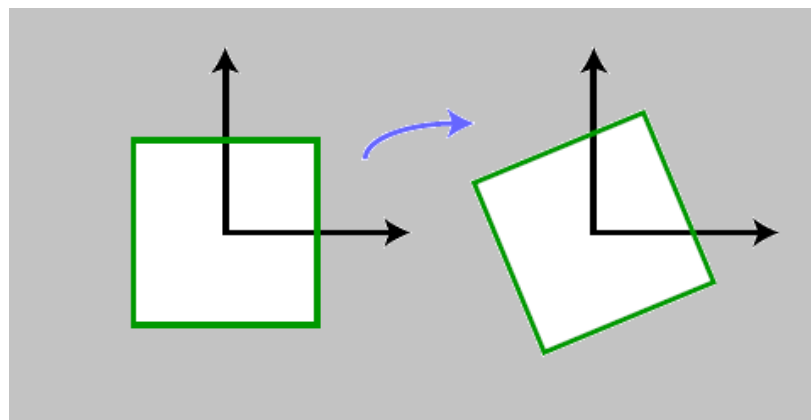


Figure 2.5. A simple rotation transformation.

2.2.2.4. Shearing

Shearing is a more complicated transformation type than translation, scaling and rotation transformations. From a transformation point of view, shearing is a linear map that transports each point in fixed direction by an amount proportional to its

signed distance from a line that is parallel to that direction. The mapping that takes a point with location (x, y) to the point with location $(x+2y, y)$ is a good example of shearing. We know that the displacement is horizontal, the fixed line is x-axis and the signed distance is the y coordinate. It is important to figure out that the points on opposite sides of the reference line are changed in an opposite direction.

Shearing transformation must not be confused with rotation transformation, shearing distorts the geometry of the figure. For instance shearing change squares to parallelograms and change circles to ellipses. One common property of both rotation and shearing is that both of them preserve areas of the images. If we consider point $P(x, y)$ the new point after shearing $P'(x', y')$ is;

Horizontal Shear

$$\begin{bmatrix} x' \\ y' \end{bmatrix} = \begin{bmatrix} x+my \\ y \end{bmatrix} = \begin{bmatrix} 1 & m \\ 0 & 1 \end{bmatrix} \begin{bmatrix} x \\ y \end{bmatrix}. \tag{2.15}$$

Vertical Shear

$$\begin{bmatrix} x' \\ y' \end{bmatrix} = \begin{bmatrix} x \\ y+mx \end{bmatrix} = \begin{bmatrix} 1 & 0 \\ m & 1 \end{bmatrix} \begin{bmatrix} x \\ y \end{bmatrix}. \tag{2.16}$$

Where m is a fixed parameter called shear factor.

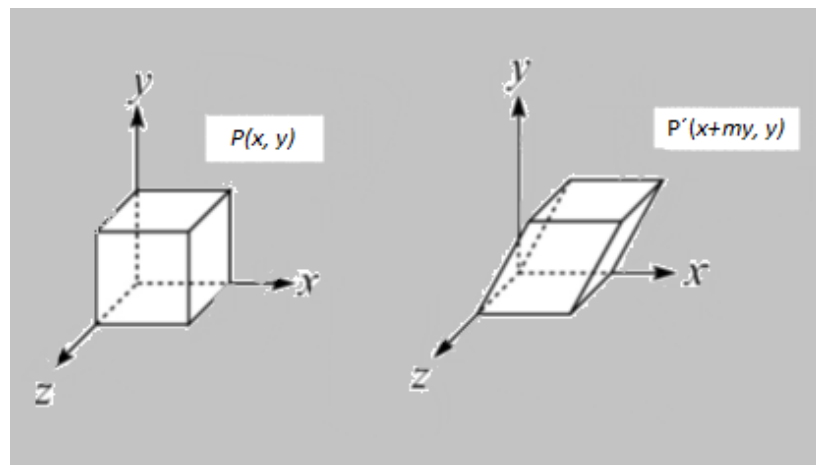


Figure 2.6. A simple horizontal shear transformation.

SUMMARY

- ✓ *Translation transformation moves a set of points a fixed distance in x and y,*
- ✓ *Scale transformation scales a set of points up or down in the x and y directions,*
- ✓ *Rotate transformation rotates a set of points about the origin,*
- ✓ *Shear transformation offsets a set of points a distance proportional to their x and y coordinates.*

2.2.3. Similarity Measure

The key similarity metric which is utilized in this thesis is known as sum of squared differences, as the abbreviated as SSD, similarity metric. This similarity metric is utilized in so many monomodal intensity registration problems and it depends on pixel intensity differences. Returning a number that indicates how well any two images are similar to each other is the goal of similarity measure. The restriction of the SSD similarity metric is that homologous images should have similar pixel intensities after accurate registration.

2.2.3.1. Sum of Squared Differences (SSD)

The expression of the SSD for image A which is Fixed Image and for image B which is Moving Image can be written as

$$SSD = \frac{1}{N} \sum_i^N |A(I) - B'(I)|^2, \quad \forall i \in A \cap B'. \quad (2.17)$$

where

A(I) = Fixed Image pixel intensity value,

B'(I) = Transformed Moving Image pixel intensity value,

N = Number of pixels in the images.

Theoretically, the SSD is said to be zero after a successful registration process however in practical it is close to zero because of the misregistrations. The SSD

metric has a limited use as mentioned previously because the fixed and moving images must be identical. Now that brain's corresponding fixed and moving MR images of the same patient are quite similar excluding the misalignments, the restriction of the SSD metric that was mentioned previously does not conflict.

2.2.4. Optimizer

The role of the optimization is to find the possible minimum value of the similarity metric. As soon as optimizer finds the minimum value of the SSD the optimization process is over. For this reason, registration process can be mathematically summarized as:

$$\min_T D[A(I), T(B(I))] \quad (2.18)$$

where

D = Similarity Metric (Cost Function),

$A(I)$ = Fixed Image,

$B(I)$ = Moving Image,

T = Transformation.

2.2.4.1. Regular Step Gradient Descend Optimizer

As for optimizer Regular Step Gradient Method is utilized at the thesis. This method was found by Cauchy in 1847. This optimization technique is among the simplest method within the optimization techniques used for image registration problems. Cauchy was the first to make use of the negative gradient direction in 1847 for minimization problems. In this method an initial trial point X_1 is chosen, which is iteratively moved along the steepest descent direction until the optimum point is found. See Figure 2.7. In a theoretical point of view, this algorithm will not end until a fixed value is achieved. The technique can be considered as an hill-climbing process. This process begins with an starting SSD guess X_k . Another estimate about the SSD X_{k+1} is made from the previous estimate X_k at each time. The difference

function is computed at all points (say, 4×4) at the neighborhood of X_k . Later on the next estimate X_{k+1} is taken that minimizes the difference function.

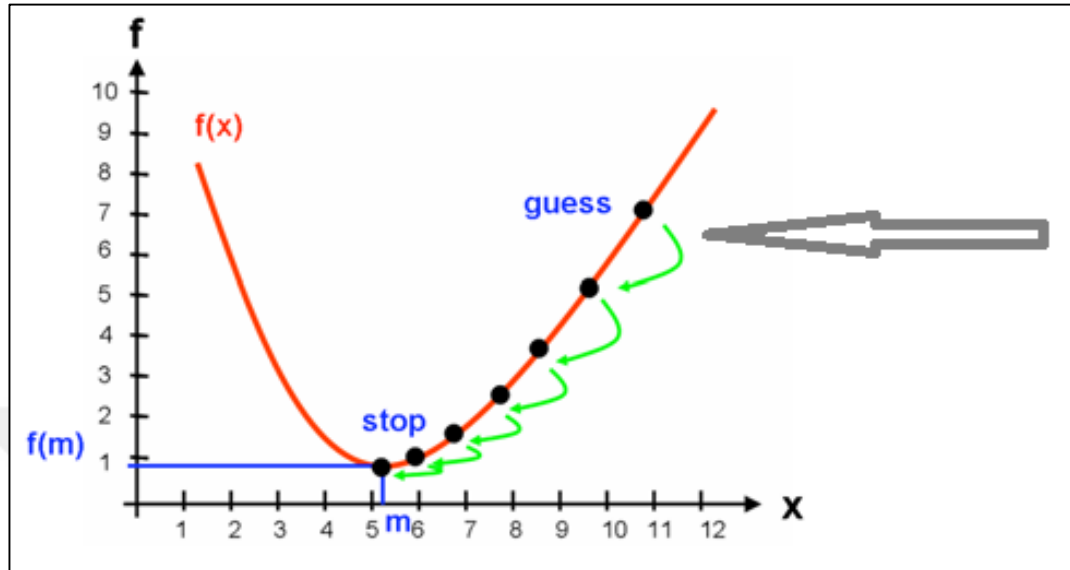


Figure 2.7. Regular step gradient descend optimizer.

2.2.5. Color Based Image Segmentation of Grown, Diminishing and Unchanged Tumor Parts using $L^*a^*b^*$ Color Space

One of the simplest methods for image segmentation is pixel clustering which is obtained by adjusting each pixel with its clustering. There are many different color spaces which have been introduced that describe the colors or gamut which can be displayed, analyzed or interpreted by electronic devices. CIE $L^*a^*b^*$ color space is commonly considered and known as the color-opponent space. In this study the purpose of using CIE $L^*a^*b^*$ color space is to establish a space which can be calculated using simple formulas from the XYZ (RGB) color coordinate system. The advantage of CIE $L^*a^*b^*$ space is that it is more perceptually uniform than XYZ space. The meaning of perceptually uniform is that a simple difference in a color value shall result in a same amount of difference in visual appearance. CIE $L^*a^*b^*$ is the most complete color space specified by the International Commission on Illumination (CIE). It contains and identifies the whole colors which are said to be visible to the naked human eye. The nonlinear relations for L^* , a^* , and b^* are intended to mimic the nonlinear response of the eye [75].

In CIE L*a*b* color space, the vertical axis L* stands for ‘‘Lightness or Luminosity’’ and its range is 0-100. The first horizontal axis which is represented by a* stands for colors fall along the red-green axis. The idea is that a color cannot be both red and green. In practice its range is from -128 to +127 (256 levels). The a* axis is red at one end (indicated by +a), and green at the other end (indicated by -a). The other horizontal axis which is represented by b* stands for colors fall along the blue-yellow axis. The idea is again that a color cannot be both blue and yellow. In practice its range is from -128 to + 127 (256 levels). The b* axis is yellow at one end (indicated by +b), and blue at the other end (indicated by -b). Each axis’s origin is said to be zero. Zero value or a very value which is very close to zero of both a* and b* will define a neutral or near neutral. a* and b* layers contain color information whereas L* layer contains luminosity (lightness) information [76].

Considering all the properties and benefits of CIE L*a*b* up to now, it can be concluded that the difference between the two points in the CIE L*a*b* color space is exactly similar with the human visual system. Therefore, after image registration process, obtained medical images are converted to CIE L*a*b* from RGB color space. Conversion from XYZ color space to CIE L*a*b* color space is achieved using the equation 19-20.

$$\begin{pmatrix} L^* = 116f\left(\frac{Y}{Y_n}\right) - 16 \\ a^* = 500\left[f\left(\frac{X}{X_n}\right) - f\left(\frac{Y}{Y_n}\right)\right] \\ b^* = 200\left[f\left(\frac{Y}{Y_n}\right) - f\left(\frac{Z}{Z_n}\right)\right] \end{pmatrix} \quad (2.19)$$

Where,

$$f(t) = \begin{cases} t^{1/3}, & t > \left(\frac{6}{29}\right)^3 \\ \frac{1}{3}\left(\frac{29}{6}\right)^2 t + \frac{4}{29}, & \text{otherwise} \end{cases} \quad (2.20)$$

X, Y and Z are the coordinates of XYZ color space. X_n , Y_n , and Z_n are XYZ tristimulus values of the reference white point. The subscript n stands for ‘normalized’. The reason for partition off $f(t)$ function is to prevent an infinite slope at $t = 0$.

2.2.5.1. Color Differences, Delta E Differences and Tolerances

In this study color difference is used to segment grown, diminishing and unchanged tumor parts from rest of the image and from each other as well after images are registered. Color difference is a well-advised technique to compute difference (distance) between two colors in color based image segmentation science. Color difference is a kind of metric which actually provides Euclidean distance. Delta E was defined by The International Commission on Illumination (CIE) and represented by ΔE which generally indicates color difference. The higher the ΔE , the bigger the difference between two colors in comparison. Theoretically, for average human vision a ΔE less than 1 is said to be indistinguishable on the condition that colors are not adjacent to each other. This means that color difference of less than 1 is hardly distinguishable by average human vision. a ΔE value between 3 and 6 is supposed to be moderate [75]. ΔE is computed using equation 21.

$$\Delta E = \sqrt{(L_2^* - L_1^*)^2 + (a_2^* - a_1^*)^2 + (b_2^* - b_1^*)^2} \quad (2.21)$$

(L_1^*, a_1^*, b_1^*) and (L_2^*, a_2^*, b_2^*) are two points having three components: L^* , a^* , b^* in three-dimensional CIE $L^*a^*b^*$ color space.

Tolerance means that how a set of colors is close to a specified reference point. Now that the distance in $L^*a^*b^*$ color space is perceptually uniform, tolerance will be defined as the set of colors whose difference to the reference point is smaller than noticeable-difference threshold. This tolerance value will specify the cluster of similar colors, i.e. pixel values. Tolerance value is a quality control for segmenting colors from each other, hence shows difference (distance) for color and lightness.

The whole process including image registration and image segmentation is summarized as follows:

Proposed Algorithm:

Step 1: Read the MR images of the patient which contains brain tumor taken at a previous time and save as Fixed Image. Read the MR image of the same patient which contains brain tumor taken at a later time and save as Moving Image.

Step 2: Register Fixed and Moving Images using similarity metric and optimizer defined previously.

Step 3: Save Fused (registered) image.

Repeat Steps 1-3 for all tumor associated MR scans of the patient brain.

Step 4: Convert Fused medical images from RGB color space to CIE $L^*a^*b^*$ color space using equations 19-20. In CIE $L^*a^*b^*$ color space, the vertical axis L^* stands for ‘Lightness or Luminosity’. The first horizontal axis which is represented by a^* stands for colors fall along the red-green axis. The other horizontal axis which is represented by b^* stands for colors fall along the blue-yellow axis.

Step 5: Draw free-hand irregularly shaped region to specify a color (i.e. anatomic parts: grown tumor, diminishing tumor or unchanged tumor).

Step 6: Compute Color Difference (Delta E) for every pixel in the image between that pixel's color and the average CIE $L^*a^*b^*$ color of the drawn region using equation 21.

Step 7: Specify the Tolerance Value according to sensitivity your work needs. Tolerance value is a quality control for segmenting colors from each other, hence shows difference (distance) for color and lightness. This is a number that indicates how close to that color would the user like to be. The algorithm then will find all pixels within that computed Delta E of the color of the drawn region.

Step 8: Categorize each pixel using nearest neighbor idea which tells that the smallest distance means similar colors, hence similar anatomic parts.

Step 9: Create new image that segment the original image by color. Green color shows tumor which has been growing with time. Magenta color, on the other hand, shows tumor which has been diminishing parts with time and lastly white color shows unchanged brain tumors.

Step 10: Compute the area of each color (each anatomic part) in segmented image.

Repeat Steps 4-10 for all Fused (registered) images.

Step 11: Add all the results came from Step 10 to compute volume of grown brain tumor, diminished brain tumor and unchanged brain tumor.

CHAPTER 3

EXPERIMENTAL RESULTS

The data has been used from RIDER Neuro MRI project from The Cancer Imaging Archive (TCIA) database [77,78]. RIDER Neuro MRI contains imaging data on 19 patients with recurrent glioblastoma who underwent repeat imaging sets with SIEMENS manufacturer. All 19 patients underwent whole brain 3D FLASH imaging in the sagittal plane after the administration of Magnevist on the same 1.5T imaging magnet. For this sequence, the Frequency was 63.676694, the TR was 6000 ms, TE 353 ms, and TI 2200ms; 180 degree flip angle, 1 signal average, matrix 256 x 216; 1 mm isotropic voxel size. The patients' head position was Head First-Supine.

Figures 3.1 (Fixed Image) and 3.2 (Moving Image) are just two MR images of a patient brain that has brain tumor. Tumors are marked with red arrows in the associated images. These MR images are taken at two different times. Figure 3.1 and 3.2 are just one scan of the patient acquired at different times. However registration process has been applied to all scans which have brain tumor. In this patient 30 scans of the patient brain have brain tumor. Slices thickness between scans is 1mm which is a perfect thickness for tumor analysis. It is investigated experimentally that in the case of tumor changing, how much brain tumor grows, how much brain tumor diminishes, or how much brain tumor stays the same using color information. Green parts shows tumor which has been growing with time. Magenta parts, on the other hand, shows tumor which has been diminishing parts with time and lastly white parts are unchanged brain tumors.

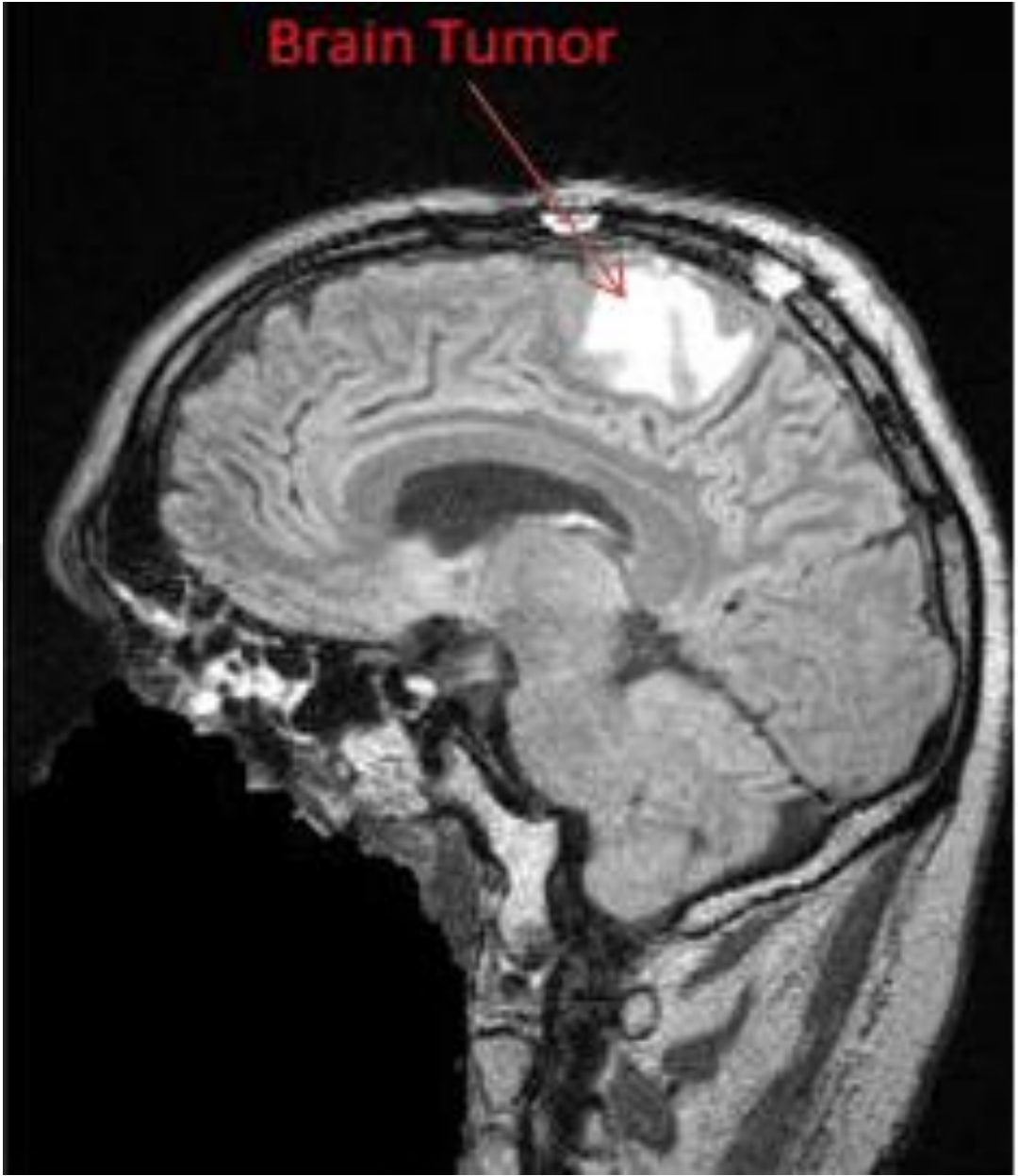


Figure 3.1. Fixed image.

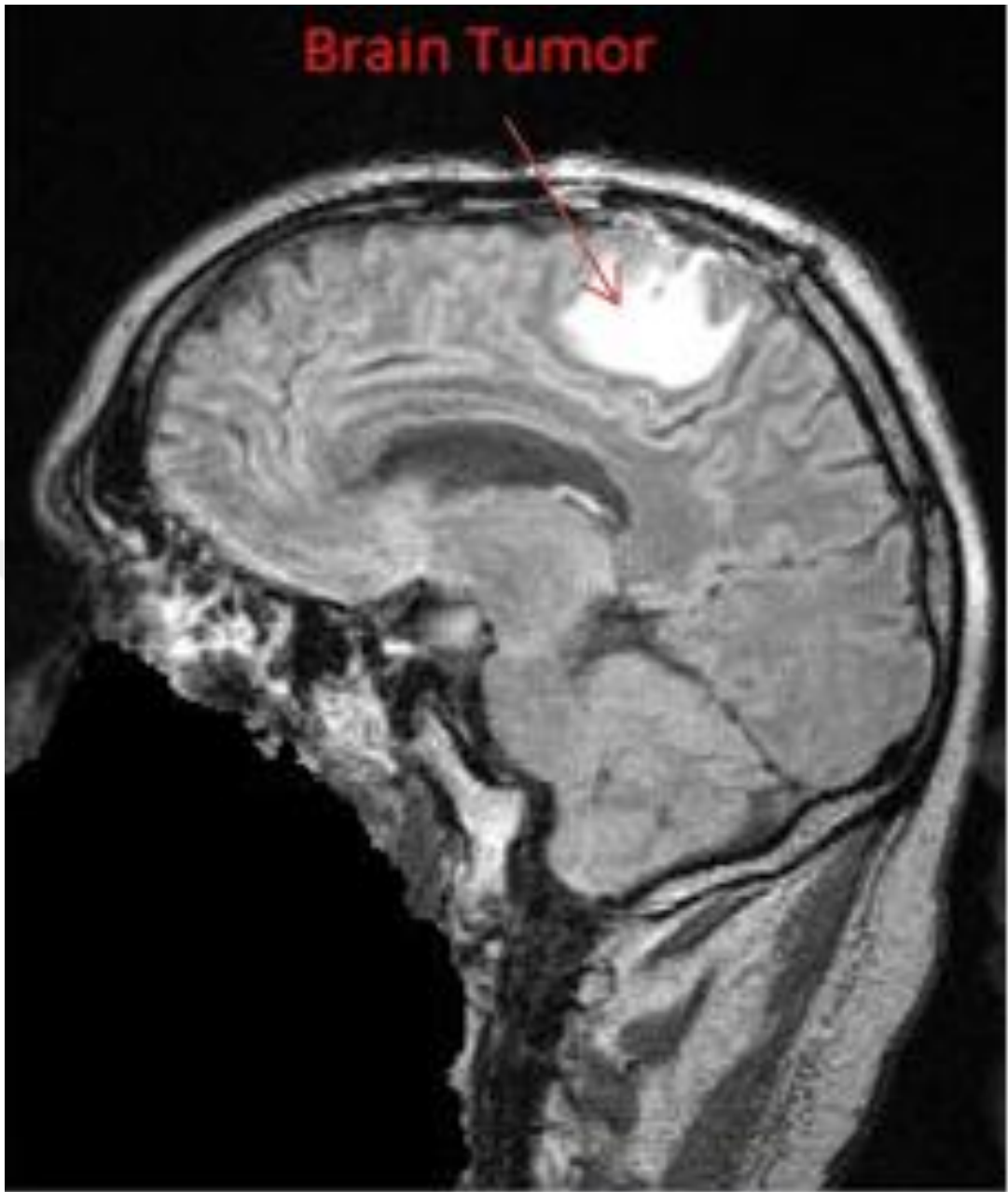


Figure 3.2. Moving image.

Figure 3.3 is just overlapping of two scans. Misregistration of the scans is quite obvious. Misregistration between two scans is marked with red arrows as well. Figure 3.4 is registration result. In figure 3.4, it can be seen that distortions which is called misregistration is removed. The remaining variations are changes which are of interest; they are therefore not distortions, they are tumor changes which are desired to be detected. These important changes are marked with red arrows. Green parts shows tumor which has been growing with time. Magenta parts, on the other hand,

shows tumor which has been diminishing parts with time and lastly white parts are unchanged brain tumors. This process has been applied to all 30 scans and results can be seen in Figure 3.7 and Figure 3.8.

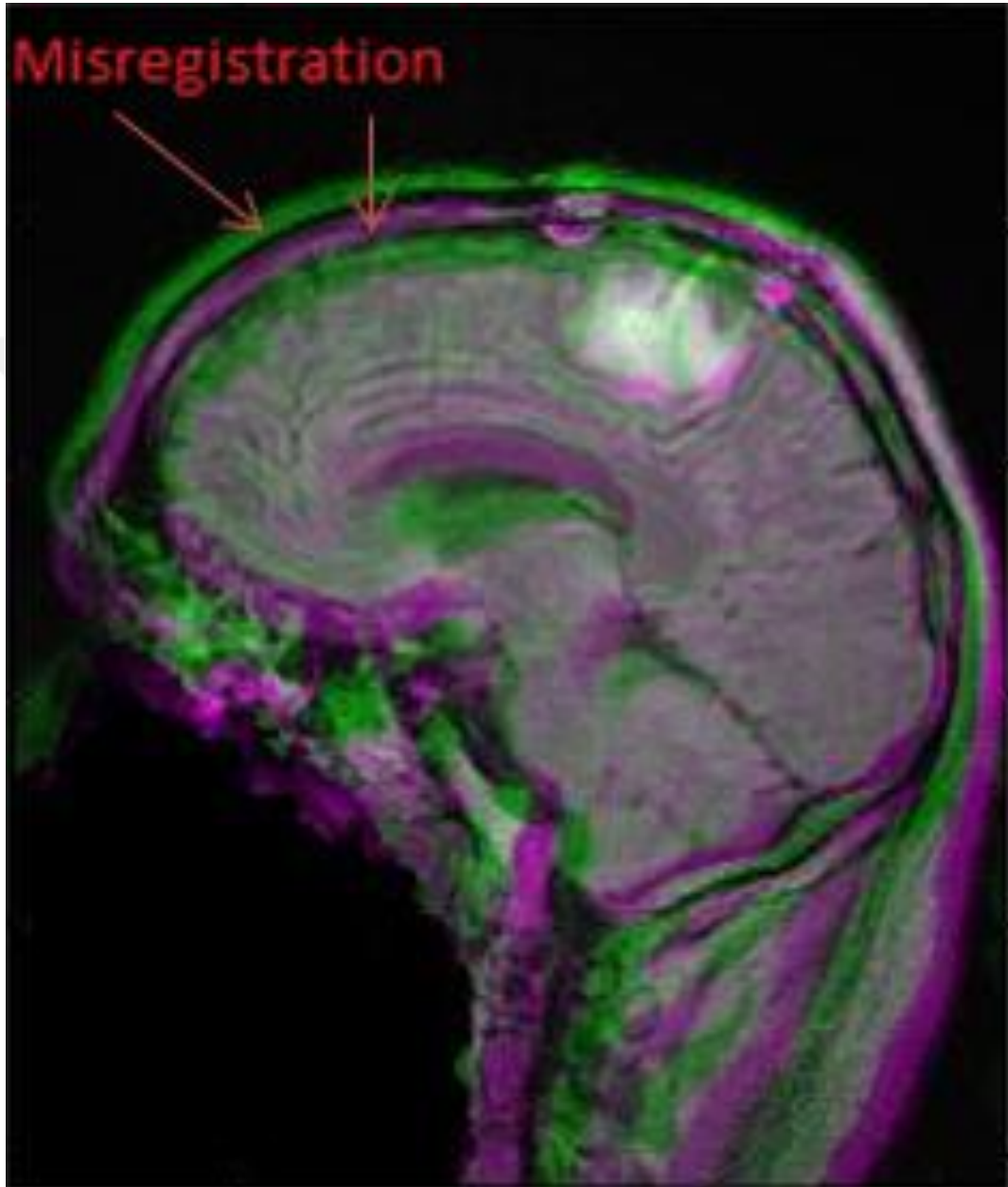


Figure 3.3. Overlapping result.

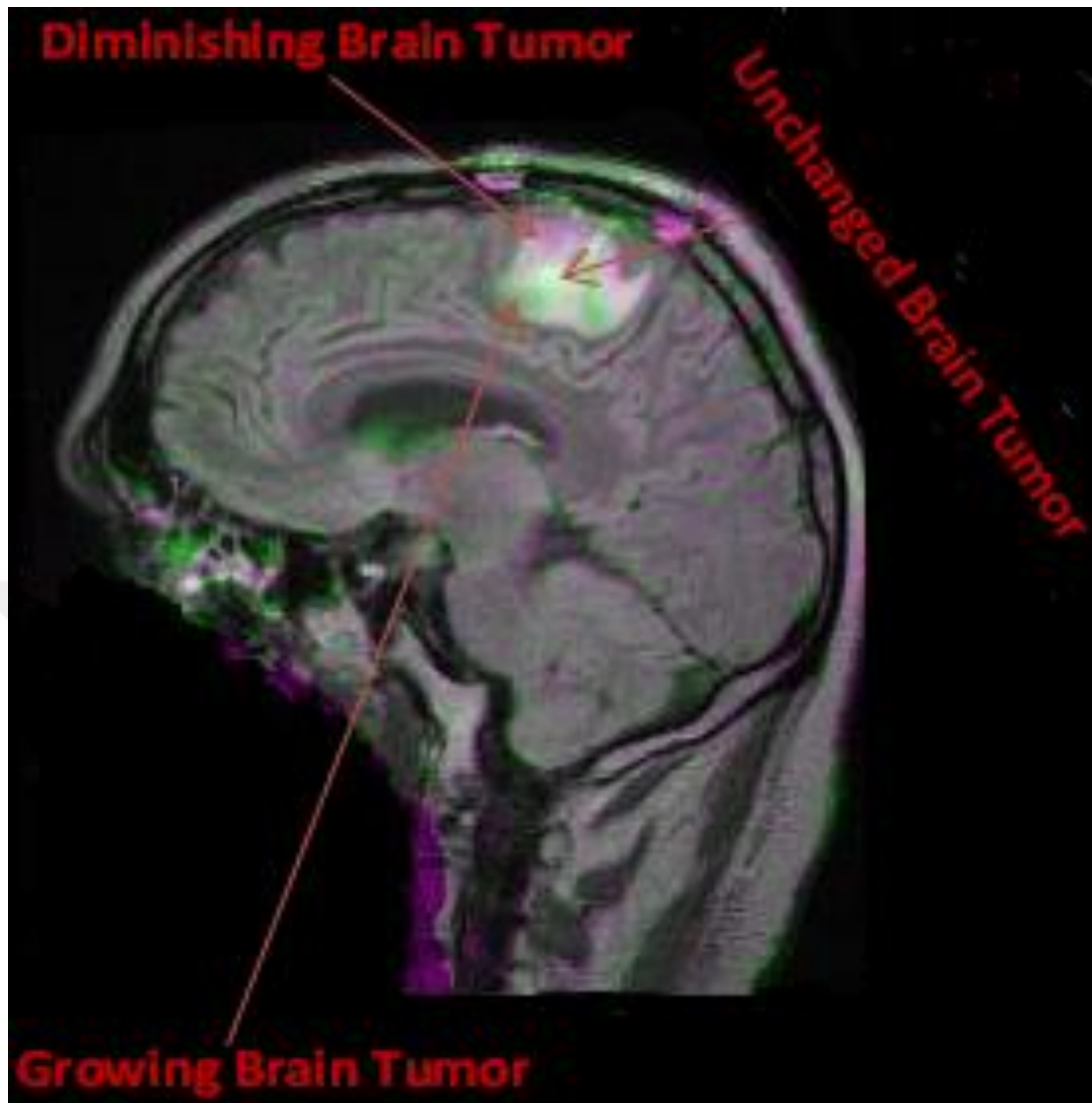


Figure 3.4. Registration result.

Segmented tumor after registration process is individually indicated in Figure 3.5. Figure 3.6 is filtering result of segmented tumor image. Figure 3.6 is necessary to compute area (hence volume) of diminished tumor part, growing tumor part and unchanged tumor part on an individual basis.

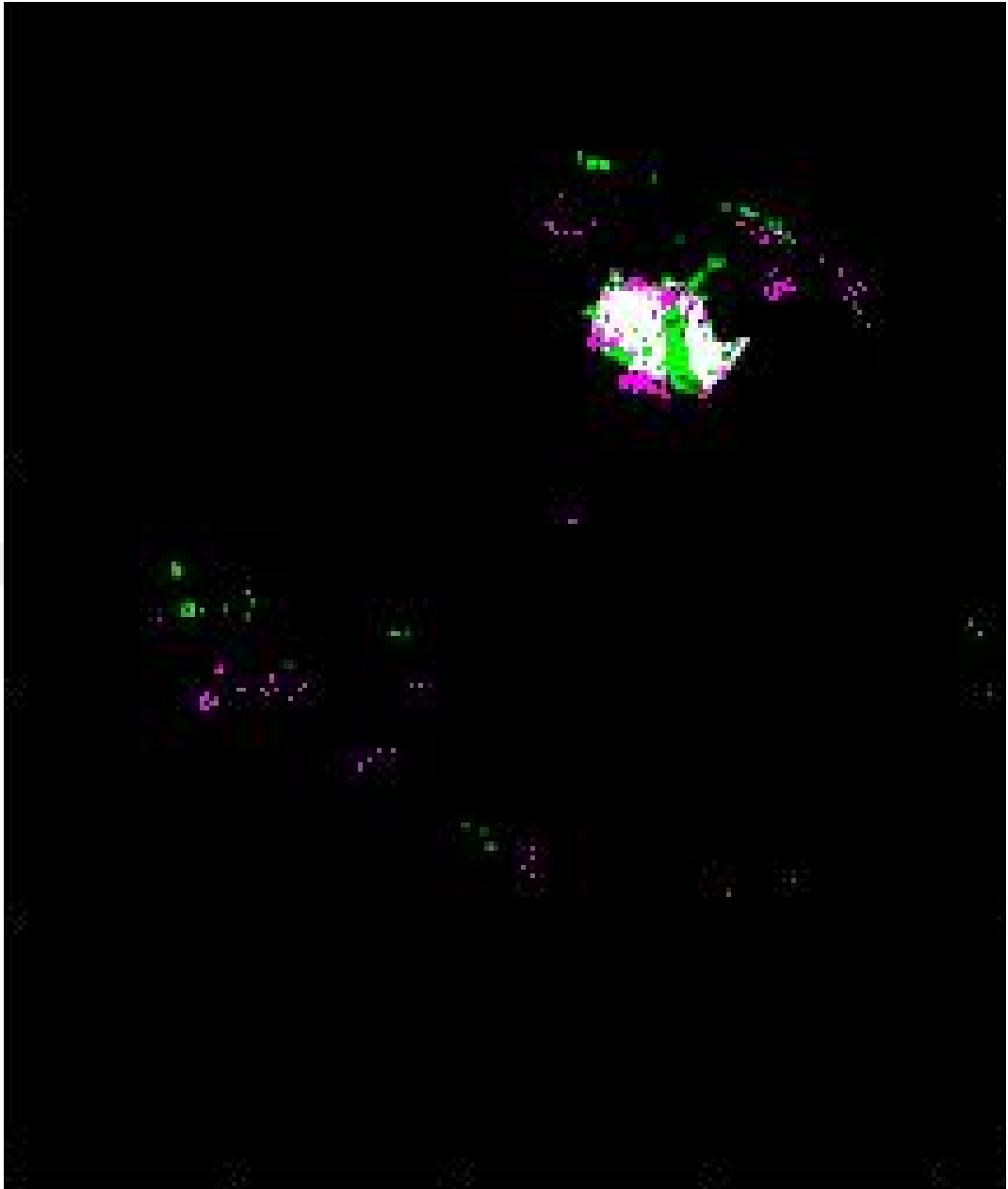


Figure 3.5. Segmented tumor.

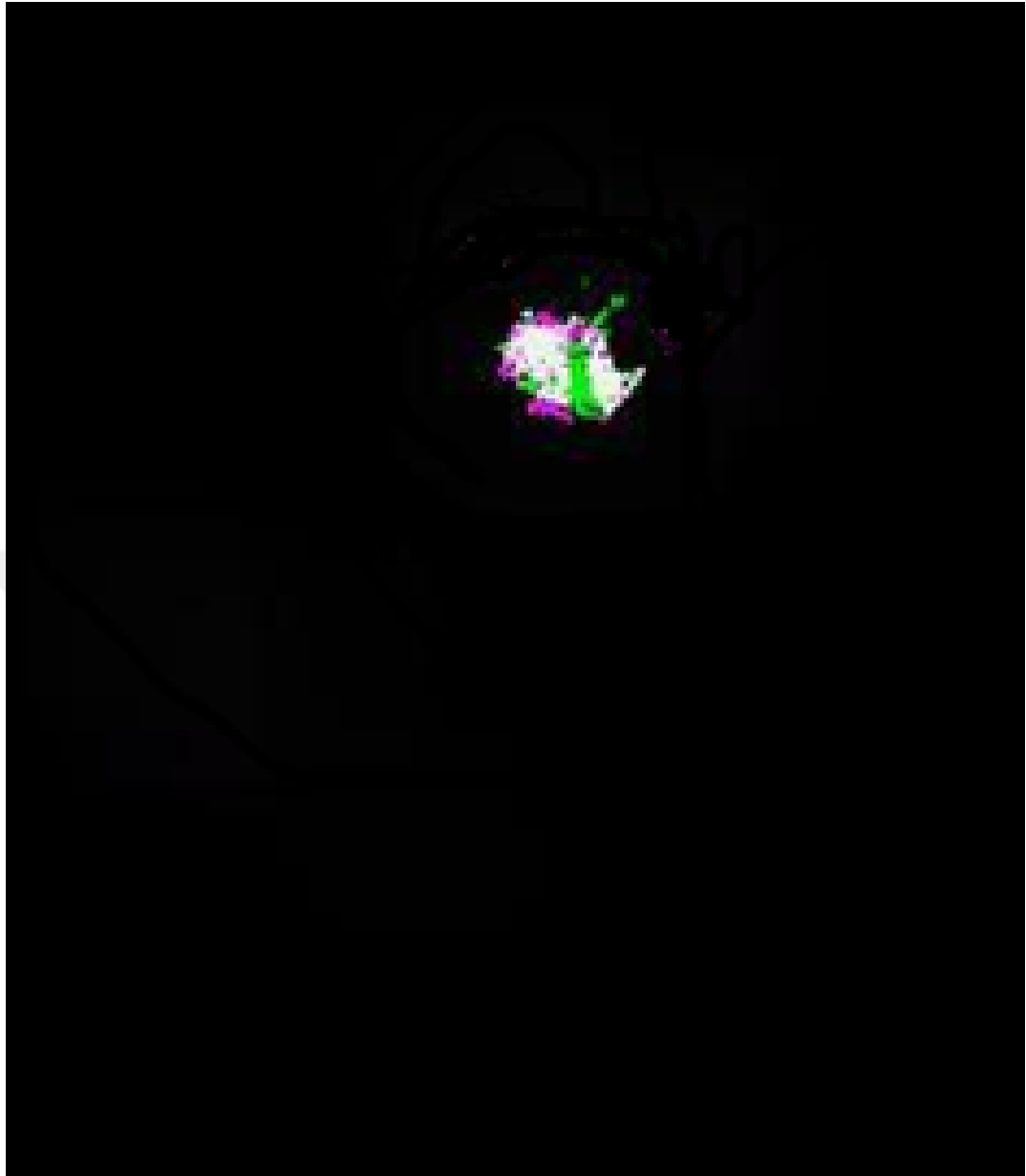


Figure 3.6. Segmented tumor after filtering.

Scores related to SSD metric is tabulated in Table 3.1 when the iteration number increases the better match is achieved. Therefore, the golden rule is that the lower the SSD, the better registration process is. Looking at the Table 3.1 it is seen that the best match is found at the Iteration Number 86. At 86th iteration number the value of SSD is 286.2024 whereas SSD number starts with 1627.2952 at 1st iteration number. On the other hand, time required for the registration increases with maximum iterations. Hence registration process takes longer time when iteration number increases.

Table 3.1. SSD results with respect to iteration number.

Iter.	SSD	Iter.	SSD	Iter.	SSD	Iter.	SSD
1	1627.2952	26	321.2599	51	286.8984	76	287.2046
2	1268.3555	27	317.4207	52	286.8578	77	286.6178
3	1584.4344	28	314.0301	53	286.6623	78	286.5840
4	5242.0876	29	310.8376	54	286.6876	79	286.5539
5	2098.3634	30	307.9623	55	286.7207	80	286.6160
6	1851.5011	31	305.6251	56	286.6427	81	286.5475
7	1525.9047	32	303.2605	57	286.5345	82	286.7101
8	1354.2674	33	300.5287	58	286.5914	83	286.6453
9	834.4523	34	298.3436	59	286.3135	84	286.7862
10	665.7449	35	296.8114	60	286.6338	85	286.8951
11	617.4345	36	294.9558	61	286.2620	86	286.2024
12	584.5832	37	293.3388	62	286.3391	87	CONVERGE
13	550.9578	38	292.7274	63	286.7855	88	CONVERGE
14	520.9090	39	290.8807	64	287.3632	89	CONVERGE
15	489.3432	40	291.0479	65	290.5421	90	CONVERGE
16	461.6606	41	294.3186	66	286.9279	91	CONVERGE
17	432.3264	42	301.4828	67	286.4376	92	CONVERGE
18	409.9917	43	302.8219	68	286.2334	93	CONVERGE
19	386.5456	44	290.8027	69	286.2593	94	CONVERGE
20	386.8915	45	287.8876	70	286.3713	95	CONVERGE
21	484.6777	46	287.7257	71	286.3901	96	CONVERGE
22	579.0272	47	287.5535	72	286.4022	97	CONVERGE
23	433.4253	48	287.3056	73	286.4613	98	CONVERGE
24	338.2038	49	287.1376	74	286.8364	99	CONVERGE
25	325.1858	50	287.1037	75	286.6227	100	CONVERGE

As stated before the process explained until this point has been implemented to all tumor associated part of the brain. For first patient this number was 30 scans. For demonstration, result of 16 scans is shown in Figure 18 and corresponding tumors are shown in Figure 3.8.

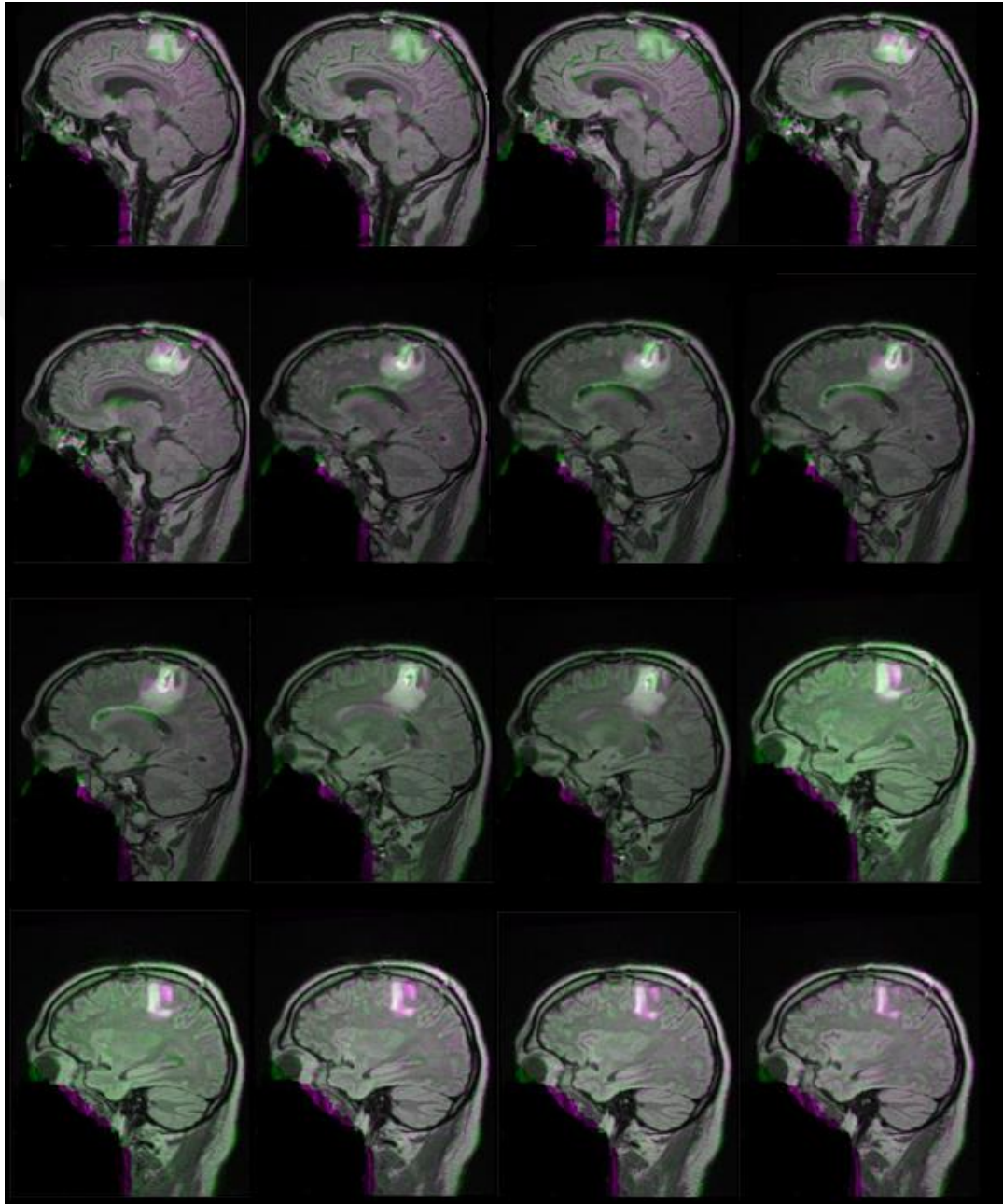


Figure 3.7. Segmented tumor (first patient).

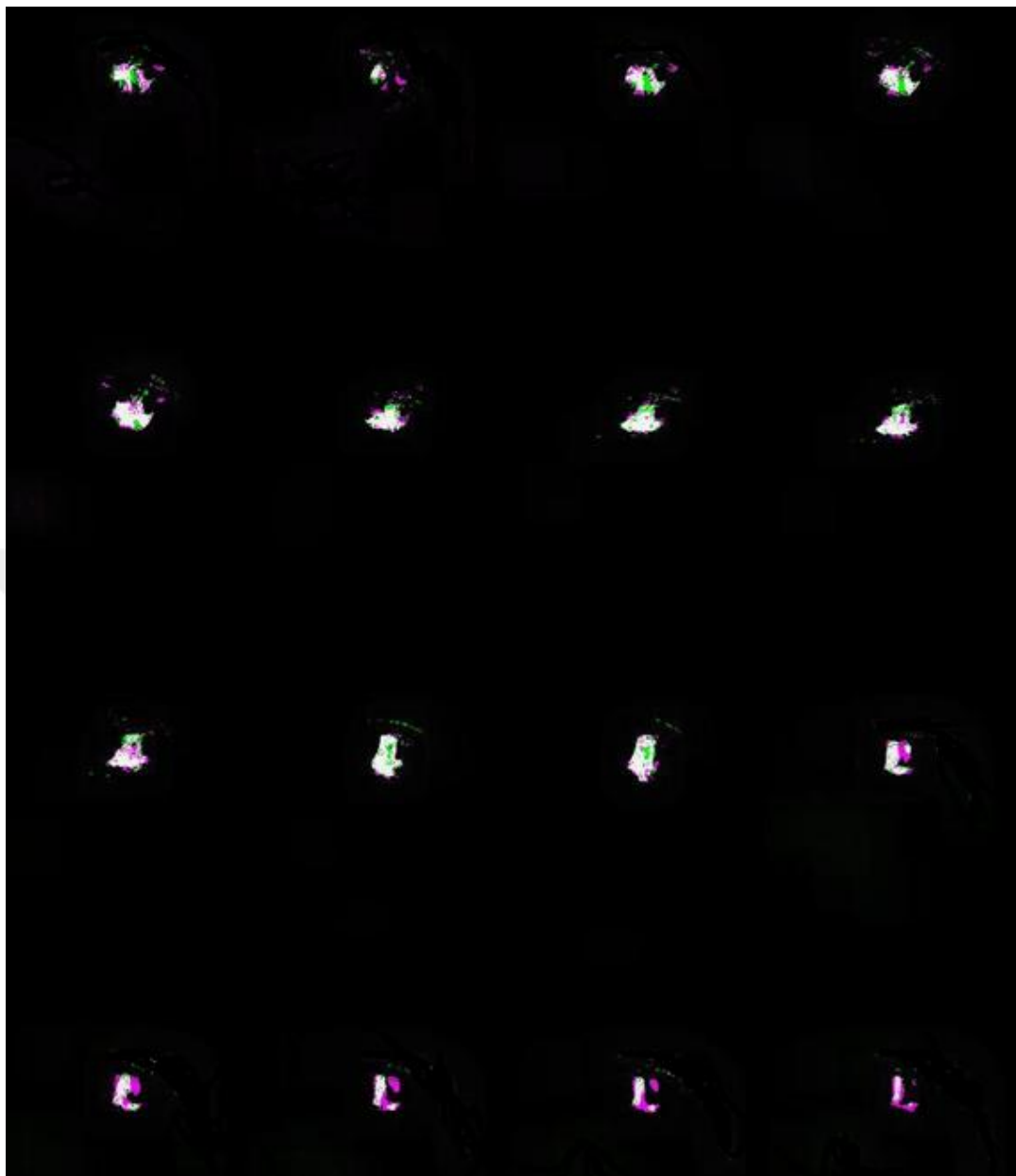


Figure 3.8. Segmented tumor (first patient).

Results for the second patient are shown in Figure 3.9 and Figure 3.10. For second patient, number of scans which are tumor associated part of the brain was 24. Registration process has been applied to 24 scans. For demonstration, result of 16 scans is shown in Figure 3.9 and corresponding tumors are shown in Figure 3.10.

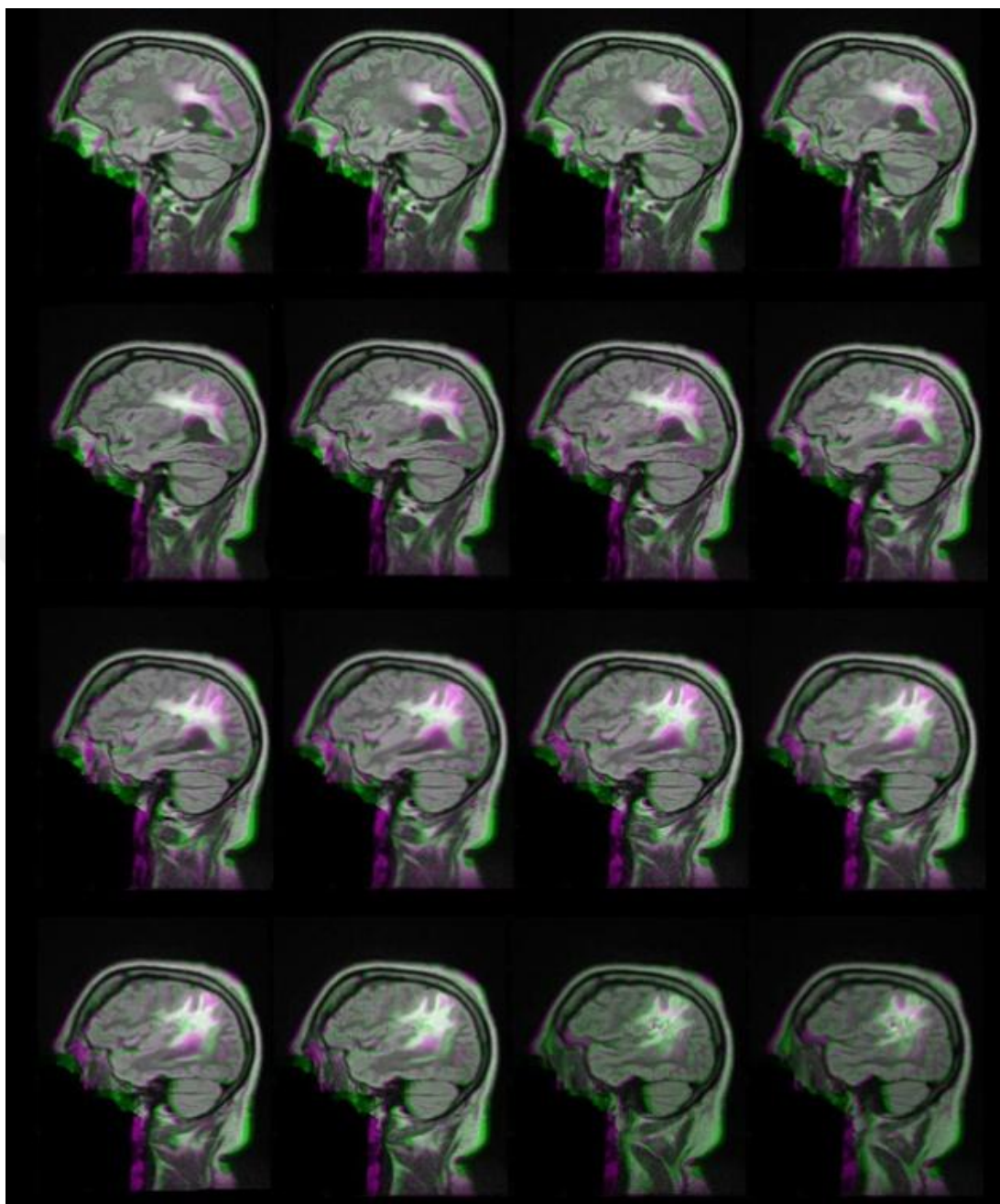


Figure 3.9. Segmented tumor (second patient).

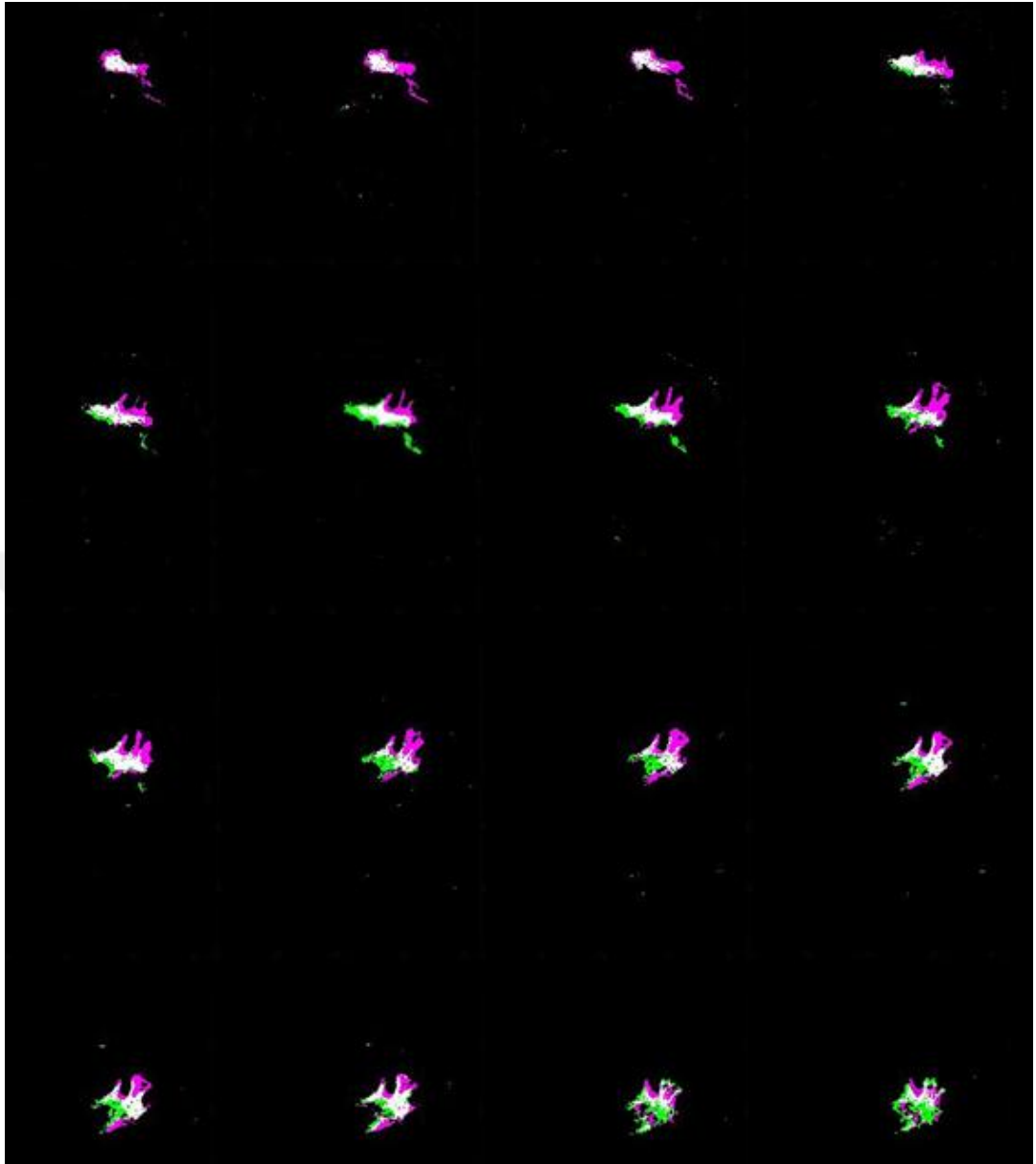


Figure 3.10. Segmented Tumor (second patient).

Table 3.2 shows volume measurement results for both mathematical models and medical image registration model. Table 3.2 is comparison of the proposed method with other standard methods. For tumor volume evaluation, there exist important mathematical models. Various studies show that three dimensional fundamental shape of brain tumor is hemi-ellipsoid. Table 3.2 shows results for 12 mathematical formula and medical image registration-segmentation method. Through these mathematical formulas $\frac{\pi}{6} * L * W * H$ is the most used formula for tumor size variation volume measurement. Results of mathematical formulas can vary from

formula to formula. Results of tumor volume vary between 72654 mm³ and 1853 mm³. Through these mathematical formulas $\frac{\pi}{6} * L * W * H$ is the most used formula for tumor size variation volume measurement and with this formula result is found to be 36659 mm³. Medical image registration-segmentation result is found to be 36154 mm³. This proves that medical image-registration method is not also between the true ranges but also is very close to the best formula. In reality medical image registration-segmentation formula gives better result than all mathematical formulas including $\frac{\pi}{6} * L * W * H$ formula. The reason is that all mathematical formulas make some assumption when measuring tumor volume. However medical image registration-segmentation method does not make any assumption. It computes each MR scan with 1 mm thickness and adds all results to compute volume. This gives the most real volumes for tumor. Besides, growing tumor part, diminishing tumor part and unchanged tumor part are also possible just for medical image registration-segmentation method. It is quite obvious that measuring the brain volume from 1D or 2D introduces further possibilities of errors in to the measurement since 1D and 2D is based on choosing maximum diameter and maximum area and so on, which is not objective but subjective. The results show that automatic 3D techniques are obviously needed for the sake of objective and are much more meaningful from a clinical point of view.

Table 3.2. Tumor volume measurement formulas and results.

Formula Used	Previous Tumor Volume (mm ³)	Current Tumor Volume (mm ³)	Growing Tumor Volume (mm ³)	Diminishing Tumor Volume (mm ³)	Unchanged Tumor Volume (mm ³)	Difference (mm ³)
<i>Medical Image Registration-Segmentation Method</i>	36154	31221	10345	15278	20876	(-) 4933
$\frac{\pi}{6} * L * W * H$	36659	31653	N/A	N/A	N/A	(-) 5006
$\frac{\pi}{6} * L * W^2$	34709	27689	N/A	N/A	N/A	(-) 7020
$\frac{\pi}{6} * \left[\frac{L+W}{2}\right]^3$	43678	33010	N/A	N/A	N/A	(-) 10668
$\frac{\pi}{6} * (L * W)^{\frac{3}{2}}$	42689	32379	N/A	N/A	N/A	(-) 10310
$0.4 * L * W^2$	28033	21177	N/A	N/A	N/A	(-) 6856
$\frac{4}{3} * \pi * \left(\frac{L}{2}\right)^3$	72654	45652	N/A	N/A	N/A	(-) 27012
$L * W * H$	70049	60483	N/A	N/A	N/A	(-) 9566
$L * W^2$	66322	55201	N/A	N/A	N/A	(-) 11121
$\frac{1}{2} * L * W * H$	35024	30241	N/A	N/A	N/A	(-) 4783
$\frac{1}{2} * L * W^2$	33166	27600	N/A	N/A	N/A	(-) 5566
$L * W$	1853	1565	N/A	N/A	N/A	(-) 288
$\frac{\pi}{4} * L * W$	1940	1228	N/A	N/A	N/A	(-) 712

Results for 19 patients' brain tumor size variation volumes using medical image registration-segmentation method are demonstrated in Table 3.3.

Table 3.3. Tumor size variation results for 19 patients using medical image registration-segmentation method.

Patient Number	Previous Tumor Volume (mm³)	Current Tumor Volume (mm³)	Growing Tumor Volume (mm³)	Diminishing Tumor Volume (mm³)	Unchanged Tumor Volume (mm³)	Difference (mm³)
<i>1. Patient</i>	36154	31221	10345	15278	20876	(-) 4933
<i>2. Patient</i>	24356	21967	11657	14657	18076	(-) 2389
<i>3. Patient</i>	37234	38644	15432	14022	23212	(+) 1410
<i>4. Patient</i>	18465	20087	2223	601	17864	(+) 1622
<i>5. Patient</i>	23987	29647	10002	4342	19645	(+) 5660
<i>6. Patient</i>	34123	31076	9109	12156	21967	(-) 3047
<i>7. Patient</i>	26781	25816	9081	10046	16735	(-) 965
<i>8. Patient</i>	21647	19087	184	2744	18903	(-) 2560
<i>9. Patient</i>	42790	44718	14873	12945	29845	(+) 1928
<i>10. Patient</i>	20043	25098	10055	5000	15043	(+) 5055
<i>11. Patient</i>	34981	30241	7903	12643	22338	(-) 4740
<i>12. Patient</i>	22132	27457	10048	4723	17409	(+) 5325
<i>13. Patient</i>	30483	35654	10531	5360	25123	(+) 5171
<i>14. Patient</i>	38654	33376	11411	16689	21965	(-) 5278
<i>15. Patient</i>	27908	31209	10319	7018	20890	(+) 3301
<i>16. Patient</i>	17592	20982	4237	847	16745	(+) 3390
<i>17. Patient</i>	23879	18231	2485	8133	15746	(-) 5648
<i>18. Patient</i>	30675	26783	11110	15002	15673	(-) 3892
<i>19. Patient</i>	29876	33832	13748	9792	20084	(+) 3956

CHAPTER 4

CONCLUSION

Brain tumors have been announced as one of the most fatal cancers in the western populations. World Health Organization specifies glioblastoma as WHO grade IV according to grading scheme which categorizes brain tumors between I and IV. That is why glioblastoma is chosen for investigation in this thesis. Magnetic resonance imaging has been used to monitor brain tumors and image processing techniques have been used to evaluate changes in the magnetic resonance images for a long time. In this thesis magnetic resonance imaging and image processing techniques are used to propose an objective application for the sake of monitoring glioblastoma volume changes.

A useful and effective application of medical image registration-segmentation is offered in this thesis with comparison of mathematical based methods. Intensity-based medical image registration phenomenon is used in this study. Sum of squared differences metric is used as similarity metric and regular step gradient descent optimizer is used as optimization technique. L*a*b color space image segmentation is used to segment each part of tumor. Using 3D medical image registration-segmentation algorithm, multiple scans of MR images of a patient who has brain tumor are registered with MR images of the same patient acquired at a different time so that growth of the tumor inside the patient's brain can be investigated. Tumor growthiness inside the patient's brain is successfully investigated. For the first patient, results are shown in Figure 3.7 and Figure 3.8. Grown brain tumor volume is found to be 10345 mm³, diminished brain tumor volume is found to be 15278 mm³ and unchanged brain tumor volume is found to be 20876 mm³. Process is applied to another patient and results are shown in Figure 3.9, Figure 3.10. For the second patient, grown brain tumor volume is found to be 11657 mm³, diminished brain tumor volume is found to be 14657 mm³ and unchanged brain tumor volume is found

to be 18076 mm³. Technique is implemented to 19 patients and satisfactory results are obtained and demonstrated in Table 3.3. A challenge of medical image registration-segmentation method for brain tumor investigation is that grown, diminished, and unchanged brain tumor parts of the patients are investigated and computed on an individual basis in a three-dimensional manner (3D) within the time. On the other hand, there is no possibility of mathematical based methods to computer grown, diminished and unchanged tumor parts. Mathematical based methods can compute previous tumor volume and next tumor volume. Most mathematical based methods are reasonable for tumor volume measurement but medical image registration is more accurate because it measures actual volume without making any assumptions.

This thesis study provides radiologists and/or clinicians to see the volume changes of the glioblastoma for neurologic research, diagnosis and treatment plan. Now that it is achieved to implicitly identify the related tumor change and to calculate related tumor volume change therefore neurologic research, diagnosis and treatment for the brain tumor are now applicable.

The next step for this study can be integrating this medical image registration-segmentation MATLAB software with a Digital Signal Processor (DSP) and to prepare an MR/MR registration machine to be used in clinics, hospitals, cancer imaging research centers etc. A new medical imaging/processing machine will provide added value to our medical technologies. This value added service will reduce external dependency and increase the standard of living of the humanity.

Another suggestion for the future work may be to apply this software tool to other kind of tumors because the software prepared is intensity based which means that it can be implemented to any tumor which has a different intensity from the whole intensity of the rest of the medical image.

REFERENCES

1. Bigos K. L., Hariri A. R., Weinberger D. R., "Neuroimaging genetics principles and practices 1th Ed.", *Oxford University Press*, New York, 157-158 (2016).
2. DeAngelis L. M., "Brain tumors", *Medical Progress N Engl J Med*, 114 (2): 114–123 (2001).
3. Kohler, B. A., Ward, E., McCarthy, B. J., Schymura, M. J., Ries, L. A. G., Ehemann, C., Jemal, A., Anderson, R. N., Ajani, U. A., and Edwards, B. K., "Annual report to the nation on the status of cancer, 1975–2007, featuring tumors of the brain and other nervous system", *Journal of the National Cancer Institute*, (2011).
4. Mazzara, G., Velthuizen, R., Pearlman, J., Greenberg, H., and Wagner, H., "Brain tumor target volume determination for radiation treatment planning through automated MRI segmentation.", *Int J Radiat Oncol Biol Phys*, 59 (1): 300–312 (2004).
5. Van Landeghem, F. K. H., Maier-Hauff, K., Jordan, A., Hoffmann, K. T., Gneveckow, U., Scholz, R., Thiesen, B., Brück, W., and Von Deimling, A., "Post-mortem studies in glioblastoma patients treated with thermotherapy using magnetic nanoparticles", *Biomaterials*, 30 (1): 52–57 (2009).
6. Krex, D., Klink, B., Hartmann, C., Von Deimling, A., Pietsch, T., Simon, M., Sabel, M., Steinbach, J. P., Heese, O., Reifenberger, G., Weller, M., and Schackert, G., "Long-term survival with glioblastoma multiforme", *Brain*, 130 (10): 2596–2606 (2007).
7. Scatliff, J. H. and Morris, P. J., "From roentgen to magnetic resonance imaging: the history of medical imaging", *North Carolina Medical Journal*, 75 (2): 111–113 (2014).
8. Seither, R. B., Jose, B., Paris, K. J., Lindberg, R. D., and Spanos, W. J., "Results of irradiation in patients with high-grade gliomas evaluated by magnetic resonance imaging.", *American Journal of Clinical Oncology*, 18 (4): 297–299 (1995).
9. Caudrelier, J.-M., Vial, S., Gibon, D., Kulik, C., Fournier, C., Castelain, B., Coche-Dequeant, B., and Rousseau, J., "MRI definition of target volumes using fuzzy logic method for three-dimensional conformal radiation therapy", *International Journal of Radiation Oncology* Biology* Physics*, 55 (1): 225–233 (2003).

10. Ten Haken, R. K., Thornton, A. F., Sandler, H. M., LaVigne, M. L., Quint, D. J., Fraass, B. A., Kessler, M. L., and McShan, D. L., "A quantitative assessment of the addition of MRI to CT-based, 3-D treatment planning of brain tumors", *Radiotherapy And Oncology*, 25 (2): 121–133 (1992).
11. Halperin, E. C., Bentel, G., Heinz, E. R., and Burger, P. C., "Radiation therapy treatment planning in supratentorial glioblastoma multiforme: an analysis based on post mortem topographic anatomy with CT correlations", *International Journal of Radiation Oncology* Biology* Physics*, 17 (6): 1347–1350 (1989).
12. Lee, S. W., Fraass, B. A., Marsh, L. H., Herbort, K., Gebarski, S. S., Martel, M. K., Radany, E. H., Lichter, A. S., and Sandler, H. M., "Patterns of failure following high-dose 3-D conformal radiotherapy for high-grade astrocytomas: a quantitative dosimetric study", *International Journal of Radiation Oncology* Biology* Physics*, 43 (1): 79–88 (1999).
13. Khoo, V. S., Adams, E. J., Saran, F., Bedford, J. L., Perks, J. R., Warrington, A. P., and Brada, M., "A comparison of clinical target volumes determined by CT and MRI for the radiotherapy planning of base of skull meningiomas", *International Journal of Radiation Oncology* Biology* Physics*, 46 (5): 1309–1317 (2000).
14. Sminia, P. and Mayer, R., "External beam radiotherapy of recurrent glioma: radiation tolerance of the human brain", *Cancers*, 4 (2): 379–399 (2012).
15. Ten Haken, R. K., Fraass, B. A., Lichter, A. S., Marsh, L. H., Radany, E. H., and Sandler, H. M., "A brain tumor dose escalation protocol based on effective dose equivalence to prior experience", *International Journal Of Radiation Oncology* Biology* Physics*, 42 (1): 137–141 (1998).
16. Char, D. H., Kroll, S., and Phillips, T. L., "Uveal melanoma: growth rate and prognosis", *Archives Of Ophthalmology*, 115 (8): 1014–1018 (1997).
17. Li, W., Gragoudas, E. S., and Egan, K. M., "Tumor basal area and metastatic death after proton beam irradiation for choroidal melanoma", *Archives of Ophthalmology*, 121 (1): 68–72 (2003).
18. Richtig, E., Langmann, G., Müllner, K., Richtig, G., and Smolle, J., "Calculated tumour volume as a prognostic parameter for survival in choroidal melanomas.", *Eye (London, England)*, 18 (6): 619–623 (2004).
19. Guthoff, R., "Modellmessungen zur Volumenbestimmung des malignen Aderhautmelanoms", *Graefe's Archive For Clinical And Experimental Ophthalmology*, 214 (2): 139–146 (1980).
20. Rubin, H., Arnstein, P., and Chu, B. M., "Tumor progression in nude mice and its representation in cell culture", *Journal of the National Cancer Institute*, 77 (5): 1125–1135 (1986).

21. Rubin, H., Chu, B. M., and Arnstein, P., "Selection and adaptation for rapid growth in culture of cells from delayed sarcomas in nude mice", *Cancer Research*, 47 (2): 486–492 (1987).
22. Karpagam, S. and Gowri, S., "Brain Tumor Growth and Volume Detection by Ellipsoid-Diameter Technique Using MRI Data", *International Journal of Computer Science*, 9 (2): 121–126 (2012).
23. Dempsey, M. F., Condon, B. R., and Hadley, D. M., "Measurement of tumor "size" in recurrent malignant glioma: 1D, 2D, or 3D?", *AJNR American Journal of Neuroradiology*, 26 (4): 770–776 (2005).
24. Talkington, A. and Durrett, R., "Estimating tumor growth rates in vivo", V: 1–27 (2014).
25. James, A. P., Dasarathy, B. V, and Consultant, I. F., "Medical Image Fusion : A survey of the state of the art", *Information Fusion*, 4-19 (2014).
26. Matl, S., Brosig, R., Baust, M., Navab, N., and Demirci, S., "Vascular image registration techniques: A living review", *Medical Image Analysis*, 35: 1–17 (2017).
27. Chen, M., Carass, A., Jog, A., Lee, J., Roy, S., and Prince, J. L., "Cross contrast multi-channel image registration using image synthesis for MR brain images", *Medical Image Analysis*, 36: 2–14 (2016).
28. Muenzing, S. E. A., van Ginneken, B., Murphy, K., and Pluim, J. P. W., "Supervised quality assessment of medical image registration: Application to intra-patient CT lung registration", *Medical Image Analysis*, 16 (8): 1521–1531 (2012).
29. Brock, K. K., Dawson, L. A., Sharpe, M. B., Moseley, D. J., and Jaffray, D. A., "Feasibility of a novel deformable image registration technique to facilitate classification, targeting, and monitoring of tumor and normal tissue", *International Journal of Radiation Oncology* Biology* Physics*, 64 (4): 1245–1254 (2006).
30. Kaus, M. R., Warfield, S. K., Nabavi, A., Black, P. M., Jolesz, F. A., and Kikinis, R., "Automated segmentation of mr images of brain tumors 1", *Radiology*, 218 (2): 586–591 (2001).
31. Thirion, J.-P., "Image matching as a diffusion process: an analogy with Maxwell's demons", *Medical Image Analysis*, 2 (3): 243–260 (1998).
32. Bloch, I., Colliot, O., Camara, O., and Géraud, T., "Fusion of spatial relationships for guiding recognition, example of brain structure recognition in 3D MRI", *Pattern Recognition Letters*, 26 (4): 449–457 (2005).

33. Alfano, B., Ciampi, M., and De Pietro, G., "A wavelet-based algorithm for multimodal medical image fusion", *International Conference On Semantic And Digital Media Technologies*, Genoa, Italy, 117–120 (2007).
34. Yuanyuan, K., Bin, L., Lianfang, T., and Zongyuan, M., "Multi-modal medical image fusion based on wavelet transform and texture measure", *Control Conference*, Chinese IEEE 697–700 (2007).
35. Zhang, Q. P., Liang, M., and Sun, W. C., "Medical diagnostic image fusion based on feature mapping wavelet neural networks", *Image And Graphics (ICIG'04), Third International Conference on Image and Graphics*, IEEE Computer Society 51–54 (2004).
36. Zhang, Q. P., Tang, W. J., Lai, L. L., Sun, W. C., and Wong, K. P., "Medical diagnostic image data fusion based on wavelet transformation and self-organising features mapping neural networks", *Proceedings of 2004 International Conference on Machine Learning and Cybernetics*, Shanghai, China, 5: 2708–2712 (2004).
37. Quellec, G., Lamard, M., Cazuguel, G., Cochener, B., and Roux, C., "Wavelet optimization for content-based image retrieval in medical databases", *Medical Image Analysis*, 14 (2): 227–241 (2010).
38. Havaei, M., Davy, A., Warde-Farley, D., Biard, A., Courville, A., Bengio, Y., Pal, C., Jodoin, P. M., and Larochelle, H., "Brain tumor segmentation with deep neural networks", *Medical Image Analysis*, 35: 18–31 (2017).
39. Pohl, K. M., Konukoglu, E., Novellas, S., Ayache, N., Fedorov, A., Talos, I. F., Golby, A., Wells, W. M., Kikinis, R., and Black, P. M., "A new metric for detecting change in slowly evolving brain tumors: Validation in meningioma patients", *Neurosurgery*, 68 (SUPPL. 1): 225–233 (2011).
40. Bauer, S., Wiest, R., Nolte, L.-P., and Reyes, M., "A survey of MRI-based medical image analysis for brain tumor studies", *Physics In Medicine And Biology*, 58 (13): R97–R129 (2013).
41. Angelini, E. D., Delon, J., Bah, A. B., Capelle, L., and Mandonnet, E., "Differential MRI analysis for quantification of low grade glioma growth", *Medical Image Analysis*, 16 (1): 114–126 (2012).
42. Oliveira, F. P. M. and Tavares, J. M. R. S., "Medical image registration: a review", *Computer Methods in Biomechanics and Biomedical Engineering*, 17 (2): 73–93 (2014).
43. Brown, L. G., "A survey of image registration", *ACM Computing Surveys*, 24 (4): 325–376 (1992).
44. Gao, X., Wang, C., Zhang, W., Wu, J., and Liu, H., "The Analysis and Application of Spline Interpolation for Multi-Sensor and Multi-Resolution

Image Registration", *International Geoscience And Remote Sensing Symposium (IGARSS)*, Toulouse France 7929–7931 (2003).

45. Fitzpatrick, J. M., West, J. B., and Maurer, C. R., "Derivation of expected registration error for point-based rigid-body registration", *SPIE Conference on Image Processing*, California, USA, 16–27 (1998).
46. Irmak, E., Erçelebi, E., and Ertaş, A. H., "Brain tumor detection using monomodal intensity based medical image registration and MATLAB", *Turkish Journal of Electrical Engineering & Computer Sciences*, 24: 2730–2746 (2016).
47. Li, L., Niu, T., and Gao, Y., "Mathematical Methods and Applications in Medical Imaging 2014", *Computational and Mathematical Methods in Medicine*, 2015: 1–2 (2015).
48. Gering, D. T., Nabavi, A., Kikinis, R., Hata, N., O'Donnell, L. J., Grimson, W. E., Jolesz, F. A., Black, P. M., and Wells, W. M., "An integrated visualization system for surgical planning and guidance using image fusion and an open MR.", *Journal of Magnetic Resonance Imaging*, 13 (6): 967–75 (2001).
49. Pereira, G. C., Traugher, M., and Jr, R. F. M., "The role of imaging in radiation therapy planning : Past , present , and future", *BioMed Research International*, 2014 (2): 1-9 (2014).
50. Chang, C. J., Lin, G. L., Tse, A., Chu, H. Y., and Tseng, C. S., "Registration of 2D C-Arm and 3D CT Images for a C-Arm image-assisted navigation system for spinal surgery", *Applied Bionics And Biomechanics*, 2015: 478-483 (2015).
51. Hurvitz, A. and Joskowicz, L., "Registration of a CT-like atlas to fluoroscopic X-ray images using intensity correspondences", *International Journal of Computer Assisted Radiology and Surgery*, 3 (6): 493–504 (2008).
52. Huang, X., Ren, J., Guiraudon, G., Boughner, D., and Peters, T. M., "Rapid dynamic image registration of the beating heart for diagnosis and surgical navigation", *IEEE Trans. Med. Imag.*, 28 (11): 1802–1814 (2009).
53. Galloway, R., Herrell, S., and Miga, M., "Image-Guided Abdominal Surgery and Therapy Delivery", *Journal Of Healthcare Engineering*, 3 (2): 203–228 (2012).
54. Ozsavag, E. E., Telatar, Z., Dirican, B., Saler, Omer, and Beyzadeollu, M., "Automatic segmentation of anatomical structures from CT Scans of thorax for RTP", *Computational and Mathematical Methods in Medicine*, 2014: 1–15 (2014).
55. Mendrik, A. M., Vincken, K. L., Kuijf, H. J., Breeuwer, M., Bouvy, W. H., De Bresser, J., Alansary, A., De Bruijne, M., Carass, A., El-Baz, A., Jog, A., Katyal, R., Khan, A. R., Van Der Lijn, F., Mahmood, Q., Mukherjee, R., Van Opbroek, A., Paneri, S., Pereira, S., Persson, M., Rajchl, M., Sarikaya, D., Smedby, rjan,

- Silva, C. A., Vrooman, H. A., Vyas, S., Wang, C., Zhao, L., Biessels, G. J., and Viergever, M. A., "MRBrainS challenge: online evaluation framework for brain image segmentation in 3T MRI scans", *Computational Intelligence And Neuroscience*, 2015: 1–16 (2015).
56. Zhuang, X., "Challenges and methodologies of fully automatic whole heart segmentation: a review", *Journal of Healthcare Engineering*, 4 (3): 371–408 (2013).
 57. Oliveira, F. P. M., Sousa, A., Santos, R., and Tavares, J. M. R. S., "Towards an efficient and robust foot classification from pedobarographic images", *Computer Methods in Biomechanics and Biomedical Engineering*, 5842 (February 2015): 1–8 (2011).
 58. Perperidis, D., Mohiaddin, R. H., and Rueckert, D., "Spatio-temporal free-form registration of cardiac MR image sequences", *Medical Image Analysis*, 9 (5 SPEC. ISS.): 441–456 (2005).
 59. Marinelli, M., Positano, V., Tucci, F., Neglia, D., and Landini, L., "Automatic PET-CT image registration method based on mutual information and genetic algorithms", *The Scientific World Journal*, 2012: 1–12 (2012).
 60. Peyrat, J. M., Delingette, H., Sermesant, M., Xu, C., and Ayache, N., "Registration of 4D cardiac CT sequences under trajectory constraints with multichannel diffeomorphic demons", *IEEE Transactions on Medical Imaging*, 29 (7): 1351–1368 (2010).
 61. Duay, V., Houhou, N., Gorthi, S., Allal, A. S., and Thiran, J. P., "Hierarchical image registration with an active contour-based atlas registration model", *European Signal Processing Conference*, Lausanne, Switzerland, 1-5 (2008).
 62. Studholme, C., Hill, D. L., and Hawkes, D. J., "Automated three-dimensional registration of magnetic resonance and positron emission tomography brain images by multiresolution optimization of voxel similarity measures.", *Medical Physics*, 24 (1): 25–35 (1997).
 63. Liao, S. and Chung, A. C. S., "With symmetric alpha stable filters", *IEEE Trans Med Imaging*, 29 (1): 106–119 (2010).
 64. Cho, Y., Seong, J. K., Shin, S. Y., Jeong, Y., Kim, J. H., Qiu, A., Im, K., Lee, J. M., and Na, D. L., "A multi-resolution scheme for distortion-minimizing mapping between human subcortical structures based on geodesic construction on Riemannian manifolds", *NeuroImage*, 57 (4): 1376–1392 (2011).
 65. Yazdani, S., Yusof, R., Karimian, A., Riazi, A. H., and Bennamoun, M., "A Unified Framework for Brain Segmentation in MR Images", *Computational and Mathematical Methods in Medicine*, 2015, 1-17 (2015).

66. Pluim, J. P. W., Maintz, J. B. A. A., and Viergever, M. A., "Mutual-information-based registration of medical images: A survey", *IEEE Transactions On Medical Imaging*, 22 (8): 986–1004 (2003).
67. Salvi, J., Matabosch, C., Fofi, D., and Forest, J., "A review of recent range image registration methods with accuracy evaluation", *Image and Vision Computing*, 25 (5): 578–596 (2007).
68. Wyawahare, M. V, Patil, P. M., and Abhyankar, H. K., "Image registration techniques : an overview", *International Journal of Signal Processing, Image Processing and Pattern Recognition*, 2 (3): 11–28 (2009).
69. Slomka, P. J. and Baum, R. P., "Multimodality image registration with software: state-of-the-art", *European Journal of Nuclear Medicine and Molecular Imaging*, 36 (SUPPL. 1): 44–55 (2009).
70. Schmidt, K. F., Ziu, M., Schmidt, N. O., Vaghasia, P., Cargioli, T. G., Doshi, S., Albert, M. S., Black, P. M., Carroll, R. S., and Sun, Y., "Volume reconstruction techniques improve the correlation between histological and in vivo tumor volume measurements in mouse models of human gliomas", *Journal of Neuro-oncology*, 68 (3): 207–215 (2004).
71. Feldman, J. P. and Goldwasser, R., "A mathematical model for tumor volume evaluation using two-dimensions", *Journal of Applied Quantitative Methods*, 4 (4): 455–462 (2009).
72. Tomayko, M. M. and Reynolds, C. P., "Determination of subcutaneous tumor size in athymic (nude) mice", *Cancer Chemotherapy and Pharmacology*, 24 (3): 148–154 (1989).
73. Du, X., Dang, J., Wang, Y., Wang, S., and Lei, T., "A parallel nonrigid registration algorithm based on b-spline for medical images", *Computational and Mathematical Methods in Medicine*, 2016, 1-14 (2016).
74. Irmak E., "Implementation of image processing techniques for tumor progression purposes in clinical application", *IEEE 2nd International Conference on Signal and Image Processing*, Singapore, Singapore, 1-4 (2017).
75. Baldevbhai, P. J. and Anand, R. S., "Color image segmentation for medical images using L * a * b * color space", *Journal of Electronics and Communication Engineering*, 1 (2): 24–45 (2012).
76. Rathore, V. S., Kumar, M. S., and Verma, A., "Colour based image segmentation using L * A * B * colour space sased on genetic algorithm", *International Journal of Emerging Technology and Advanced Engineering*, 2 (6): 156–162 (2012).

77. Barboriak, D., "Data from RIDER_NEURO_MRI.", *The Cancer Imaging Archive*. [Http://doi.org/10.7937/K9/TCIA.2015.VOSN3HN1](http://doi.org/10.7937/K9/TCIA.2015.VOSN3HN1), (2015).
78. Clark, K., Vendt, B., Smith, K., Freymann, J., Kirby, J., Koppel, P., Moore, S., Phillips, S., Maffitt, D., Pringle, M., Tarbox, L., and Prior, F., "The Cancer Imaging Archive (TCIA): Maintaining and Operating a Public Information Repository", *Journal of Digital Imaging*, 26 (6): 1045–1057 (2013).



RESUME

Emrah IRMAK was born in 1988 in Mardin, Turkey. He completed his primary and secondary education in his hometown, Nusaybin. He completed his high school education in Mardin Anatolia High School in 2007. Emrah Irmak started his Bachelor's degree in Electrical and Electronics Engineering at the Faculty of Engineering, Gaziantep University, Gaziantep, in 2007. The language of the study was English. In 2011 he earned scholarship for continuing his bachelor studies as an Erasmus student at the Opole University of Technology in Opole, Poland. He enrolled in Electrical Engineering, Automatic Control and Informatics study programme. The studies were summoned in January, and he completed his Erasmus studies in June 2011. Immediately after that he continued his bachelor education in Gaziantep University and he was graduated from Gaziantep University in January 2012. As soon as he finished his bachelor he started his Master Education in the same university and same department in Gaziantep. Emrah Irmak completed his Master's Degree in June 2014. The master thesis was titled: "Application of Monomodal Intensity-based Medical Image Registration Technique on Brain Tumor Growthiness Investigation". The language of the study was English. He started pursuing his PhD degree in September 2014. He completed his doctoral studies successfully in January 2018. The doctoral thesis was titled: "3 Dimensional Monomodal Intensity-based Medical Image Registration for Brain Tumor Progression Analysis". From June 2012 Emrah Irmak is a part of Department of Biomedical Engineering at the Faculty of Engineering of Karabuk University as a Research Assistant.

CONTACT INFORMATION

Address : Karabuk University Engineering Faculty, Department of Biomedical Engineering 4th Floor, Room No: 427

E-mail : emrahirmak@karabuk.edu.tr; emrah.2@hotmail.com